Review

Lanthanide Complexes with Tripodal Ligands

Kira E. Vostrikova [1,*]

[1] Nikolaev Institute of Inorganic Chemistry, Siberian Branch, Russian Academy of Sciences, 630090 Novosibirsk, Russia;

* Correspondence: vosk@niic.nsc.ru

Abstract: The main property of tripodal ligands is the predictable type of coordination. Homo- and heteroleptic lanthanide complexes with tripodal ligands are a representative class of compounds. However, despite the fact that many of them are paramagnetic their magnetic behavior is poorly understood. This is because their photophysical and catalytic properties have been more attractive. In the present review, we are trying to summarize the available structural information and extremely few data on magnetic properties in order to draw some conclusions about the prospective of tripods using in the design of quantum molecular magnets based on Ln ions. We would like to draw the reader's attention to the fact that despite the consideration of a large part of the currently known lanthanide compounds with tripodal ligands, this review is not exhaustive. However, our goal was to draw the attention of researchers to the fact that a whole niche of air-stable Ln complexes remained outside the attention of magnetochemists and theoreticians.

Keywords: tripodal ligands; lanthanides; single-molecule magnets; single-ion magnets; axiality

1. Introduction

Rational design of coordination compounds with specific physical properties is a challenging task for the synthetic chemists. Chemical engineering can be highly specialized (focusing on improving a specific property) or it can be aimed at preparing polyfunctional materials. The most common objective for materials scientists is to tune the electronic properties of a compound. This can be achieved by varying the ligand environment of the central atom: geometry of the polyhedron and the ligand field strength. The latter is mainly defined by the donor atoms composition, whereas the former depends not only on the geometry of the ligand, but also on the predictability of its coordination mode. The organic tripod molecules having the donor atoms on each of their three legs are the best choice for the chemical design of the different complexes with a given geometry. Moreover, the latter can be easily varied by using the methods of synthetic organic chemistry. Therefore, it is not surprising that tripodal ligands are widely used in various fields of applied coordination chemistry such as catalysis [1–6], chemo sensing [7–9], photo-[10–12] and electroluminescence [11,13,14], molecular gears and motors production [15,16], biomedical applications [17–20] and molecular magnetism [12,21–24].

Although numerous high-spin molecules based on tripodal ligands (including paramagnetic ones [25–32]) and d-metal ions have been studied to date [33–42], for 4f elements such studies are mainly focused on synthesis, the structural features and photophysical properties of compounds with diamagnetic tripods, often leaving aside the study of their magnetic behavior [10,11,14,18,43–48]. The present review is devoted to the analysis of known lanthanide complexes with tripodal ligands from the point of view of their application in the field of molecular magnetism.

2. Short theoretical background

Due to slow attenuation of magnetization and existence of magnetic hysteresis of purely molecular origin, single-molecule magnets (SMMs) could offer considerable future application in the domain of spintronics, quantum computing and, especially, for use as materials for storing information at the molecular level. There are three main characteristics of SMMs. The first is the

Preprints (www.preprints.org) | NOT PEER-REVIEWED | Posted: 14 June 2023 doi:10.20944/preprints202306.0983.v1

effective energy barrier (U_{eff}) providing magnetic bistability due to spin reversal between the two ground states (GS). Highly efficient SMMs are very different in their behavior, since large U_{eff} do not ensure that magnetization is kept at the elevated temperature during a period necessary to serve as a magnetic storage. This is defined by the second characteristic called blocking temperature (T_B), which is a central claim for the implementation of SMMs in practice. Usually, the spin-lattice relaxation and quantum tunneling of magnetization (QTM) lead to the magnetization disappearance in an SMM. The first associated with spin-phonon coupling, which can manifest itself through three different mechanisms: Orbach, Raman and direct. The QTM is a temperature-independent phenomenon. A thermally assisted QTM process on excited states is also possible, through which the relaxation occurs. These processes, phonon type relaxation and QTM, described in many papers [49–51] closely related with the third SMM characteristic – relaxation time (τ). The U_{eff} value is ordinarily determined from the Arrhenius dependence of relaxation time for the Orbach process. For the main SMM's characteristic, T_B, the more common definition is that the magnetization blocking temperature is a temperature below which magnetic hysteresis is opening. The stronger the SMM coercive field and the higher the residual magnetization at zero magnetic field, the better magnetic bistability the magnetic material will exhibit. In addition, higher U_{eff} and T_B provide quantized magnetization with satisfactory suppression of spin-lattice relaxation. The T_B is now much lower room temperature, limiting possible technological applications [49–53]. Consequently, the quest for SMMs possessing large U_{eff} and T_B is a crucial issue in molecular magnetism. An important category of SMMs, lanthanide (Ln) single-ion magnets (or SIMs), are particularly promising due to their huge magnetic moments with immense magnetic anisotropy caused by a large spin–orbit coupling offered by the unquenched orbital momentum [54,55]. Improved (T_B) and (U_{eff}) are indispensable to realize their practical applications.

Almost thirty years of transdisciplinary investigations have resulted in SIMs with record U_{eff} (up to 2000 K) and T_B near liquid nitrogen temperature [56–59]. This is a result of several approaches, which have been shown that enhancing the uniaxiality of magnetic anisotropy is crucial for the design of highly performed SIMs [60–64]. The uniaxiality of SIMs can be provided by the corresponding symmetry of the coordination polyhedron. However, despite the similarity in chemical behavior (due to the shielded nature of the f-electrons) Ln^{3+} are very different in terms of electronic properties. This leads to the fact that for ions differing in electronic configurations, along with the crystal field (CF) splitting, their ligand environment must be taken into account. Among the lanthanides (Ln), the tri-valent Tb, Dy, Ho, and Er can produce large m_J ground states if the appropriate CF is provided [65]. This is due to that the electronic clouds of Ln GS have different shapes. The letter are generally subdivided into prolate and oblate spheroid types [60,66–68], which requires respectively different ligand field organization: axial for Pr, Tb, Dy, Nd and equatorial for Pm, Tm, Yb, and Er [60,69]. Thus, to increase the energy barrier U_{eff}, the symmetry of a Ln^{3+} ion environment, along with the ligand field approach (axial or equatorial), are required depending on the nature of the Ln^{+3} [70,71]. Although this provides an opportunity to design the SMM with the ground states with large magnetic moment, relaxation often occurs through excited states that have different electron densities. In addition, the energy gap separating the m_J levels (a key parameter for SMM enhancement) is difficult to forecast until a quantitative approach is applied and the mechanisms of relaxation are entirely established.

If strong intermolecular exchange interactions are absent between the mononuclear SIMs (which is precisely the case for lanthanide ions, since the magnetic electrons are on a well screened 4f shell), then the surrounding the magnetic metal ions ligand field leads to the degeneration of the $^{2S+1}L_J$ multiplets resulting in $2J + 1$ sublevels m_J. This generates a highly anisotropic ground spin state, which can be explained using quantum mechanics. However, we will not immerse the reader in the mathematical details for all types of magnetic anisotropy, since they can be found in the literature [72–74]. In regard of the fixed molecular structure, uniaxial anisotropy is important to suppress QTM and decrease thermo-assisted relaxation. In addition, a source of under barrier QTM is the transverse anisotropy caused by transverse CF that should be avoided in design of SIMs. Tong et al. [75] have studied the influence of symmetry on the transverse terms. They conclude that for the $C_{\infty v}$, C_{5h}/D_{5h}, S_8/D_{4d}, and S_{12}/D_{6d} symmetry vanish terms B_k^q ($q \neq 0$) of CF for interested Ho^{3+} ion, resulting in the

Preprints (www.preprints.org) | NOT PEER-REVIEWED | Posted: 14 June 2023 doi:10.20944/preprints202306.0983.v1

perfect uniaxial anisotropy. Thus, by adjusting the symmetry of the coordination polyhedron and the ligand environment for a particular lanthanide center, QTM in SIM can be battled.

However, even the most accurate theoretical predictions are not easy to implement in practice, since in order to obtain a coordination polyhedron with a certain symmetry, it is necessary to use ligands with a predictable manner of coordination. Therefore, when designing any SIM, it is up to synthetic chemists to find a compromise between polyhedra with uniaxial symmetry and the choice of ligands for building magnetic molecules.

Therefore, the analysis of currently known molecular mononuclear complexes containing tripodal ter- and tetradentate ligands is aimed at drawing the attention of the scientific community to the use of such ligands in the design of Ln complexes with uniaxial anisotropy. To date, approaches have been developed to choice the most suitable Ln-ion for the appropriate ligand environment, based on the shape of 4f-electron clouds (oblate or prolate) for both the ground state and the excited levels of the central atom [60,76–78].

3. Lanthanide complexes with tripodal ligands

3.1. Complexes with the pyrazolyl bearing tripodal ligand

3.1.1. Complexes with tris(pyrazolyl)borates tripodal ligands

The first and most studied coordinative tripods were the scorpionate ligands hydro-tris(pyrazolyl)borates, first obtained by S. Trofimenko [33,35]. The coordination chemistry of these negatively charged ligands mainly includes d-metal complexes [37,79,80]. In the chemistry of coordination-capacious f-elements, scorpionates are often used as capping ligands that additionally compensate for the positive charge of Ln [81–86]. In the area of molecular magnetism, the bulky hydro-tris(pyrazolyl)-borate (TPzB) is commonly employed as a capping ligand to reduce intermolecular magnetic interactions and protect the air-sensitive radical cites [87]. Besides, a number of 3d ion-based SMMs and SCMs (single-chain magnets) [88,89] have been obtained by using this approach. Unfortunately, very few Ln-TPzB complexes have been magnetically studied.

Among them three Dy^{3+} compounds: one purely homoleptic $[Dy(Tp^{Me_2})_2]I$ (**1**), one heteroleptic $(Me_4N)[DyCl_3(Tp^{Me_2})]$ (**2**) (Tp^{Me_2}=tris(3,5-dimethylpyrazolyl)borate), and one mixed type complex $[Dy(Tp^{Me_2})_2][DyCl_3(Tp^{Me_2})]\cdot CH_2Cl_2$ (**3**) are described [90]. The Dy^{3+} ions are 6-coordinate for all three complexes (Fig. 1). The $[Dy(Tp^{Me_2})_2]^+$ cation in **3** adopts a bent sandwich-type structure with a B–Dy–B angle of 169.57(3)° [90]. In the cationic part, the Dy^{3+} ion is surrounded only by N-atoms of two Tp^{Me_2}, while in the anionic part the coordination sphere of Dy^{3+} consists of three nitrogen atoms from one tripod and three chloride ions. The structural shape analysis has shown that the Dy-center in cation **3** is in an elongated trigonal antiprismatic coordination environment (Figure 1) [90]. Such a geometry has been previously found for divalent lanthanide [44,46,91].

Complex **2** contains the separate $[DyCl_3(Tp^{Me_2})]^-$ anion, which is alike to that of **3** but having Me_4N+ as a cation. Compound **1** is isomorphous to the Sm^{3+} analogue reported earlier [44]. It contains well isolated $[Dy(Tp^{Me_2})_2]^+$ and iodide ions. The cation in **1** placed in a 2/m symmetry element representing a mirror plane passing through two of the pyrazolyl rings [90]. It is noteworthy that the Dy-center in the cation **1** has a similar geometry comparatively to those of the compound **3**, but it has the following key dissimilarities: the two independent Dy–N bond distances, 2.376(2) and 2.430(3) Å, are longer compared to those of **3**; due to the crystallographic symmetry, the two planes defined by the nitrogen donor atoms of each tripod are parallel, whereas in **3** the angle between the planes is 10.53(2)°; both the Tp^{Me_2}–Dy–Tp^{Me_2} and B–Dy–B angles in **1** (178.64(2)° and 180.00(2)°), are broader than those of **3** (173.05(2)° and 169.57 (2)°), indicating that cation **1** reveals a more dense and linear structure than the cation in **3**. In conclusion, the isolated $[DyCl_3(Tp^{Me_2})]^-$ is in a alike trigonal antiprismatic coordination environment having the very similar bond distances and angles for the compounds **2** and **3** [90].

Preprints (www.preprints.org) | NOT PEER-REVIEWED | Posted: 14 June 2023 doi:10.20944/preprints202306.0983.v1

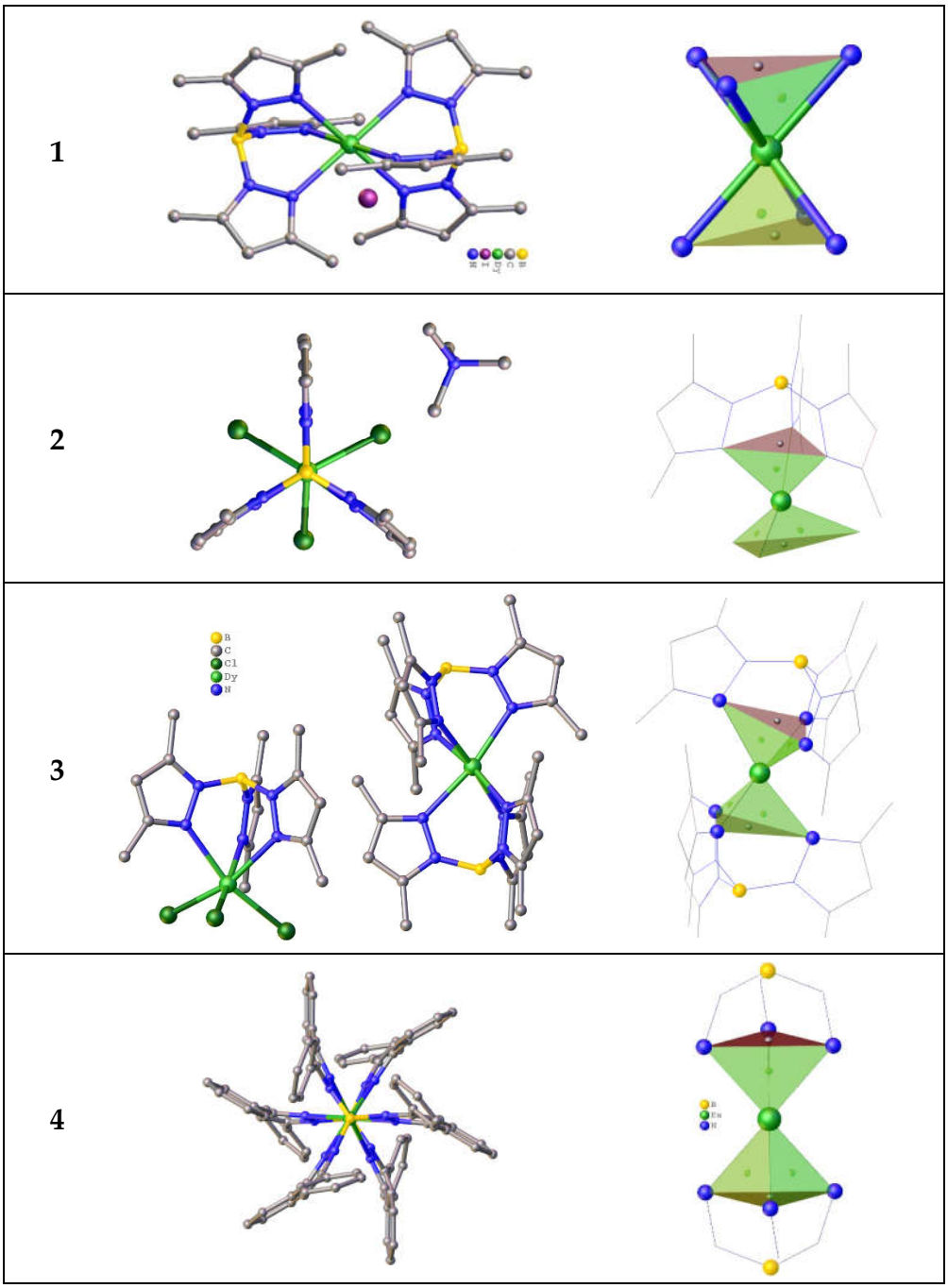

Figure 1. Molecular structures (left) and trigonal antiprismatic coordination polyhedra (right) for the compounds **1**-**4**. Hydrogen atoms are omitted. The picture was made using open crystallographic data.

Magnetic studies have shown that complex **1** displays an energy barrier U_{eff} of 13.5 K with $\tau_0 = 1.6 \times 10^{-6}$ s under a 0.08 T applied field, while **3** is a SIM with $U_{eff} = 80.7$ K and $\tau_0 = 6.2 \times 10^{-7}$ s under a zero applied field [90]. The results of the first principles CASSCF + RASSI-SO calculations correspond well the experimental magnetic measurements for **3** and **1** indicating the presence of an intermolecular dipolar interaction of ($zJ = -0.1$ cm^{-1}) in **3** [90]. The absence of SMM behavior in **1** and **2** under a zero dc field supports the conclusion that the slow magnetic relaxation observed for **1** is a result of minor changes in the coordination geometry of the Dy^{3+} ion, and/or intermolecular dipolar interactions between the anionic and cationic moieties [90]. The QTM probability of ground state for Kramers doublets is described by the crystal field (CF, B_k^q) parameters. QTM is prevailing when the non-axial terms (for which $q \neq 0$ and $k = 2, 4, 6$) are larger compared to the axial ones (for which $q = 0$ and $k = 2,4,6$). For all the Dy^{3+} ions in 1–3, there is significant transverse anisotropy and fast QTM

Preprints (www.preprints.org) | NOT PEER-REVIEWED | Posted: 14 June 2023 doi:10.20944/preprints202306.0983.v1

relaxation [90]. The cationic Dy1 units in 1 and 3, however, have relatively small temperature assisted-QTM in the first excited states. This situation can assist in magnetization relaxation via the first excited states when a dc field is applied [90].

From the point of view of the design of high-performance SIMs, it would be worth paying special attention to the recent publication by Hao Qi et all [92] devoted to the synthesis of Eu(II) compounds with bulky tris-pyrazolyl-borates. First of all, it should be noted that the obtained three complexes are stable under ordinary conditions and can be sublimated. Both of these properties are extremely important for practical applications. When extending the synthesis procedure chosen by the authors to magneto-anisotropic Ln ions, it would be interesting to test these compounds for SMM behavior. The complexes $Eu(Tp^{Ph,Me})_2$, $Eu(Tp^{Ph})_2$ and $Eu(Tp^{Ph2})_2$ are all hexa-coordinated, with six N atoms from pyrazole heterocycles. $Eu(Tp^{Ph})_2$ is isomorphous to the known compounds $Sm(Tp^{Ph})_2$ and $Yb(Tp^{Ph})_2$ [44]. The molecular structure of $Eu(Tp^{Ph2})_2$ differs from those of $Eu(Tp^{Ph,Me})_2$, $Eu(Tp^{Ph})_2$. Due to the substituents change, the structure symmetry of the compounds rises in the following order $Eu(Tp^{Ph,Me})_2 \rightarrow Eu(Tp^{Ph})_2 \rightarrow Eu(Tp^{Ph2})_2$, the latter having a higher symmetry of D_{3d}, while the others possess a "bent sandwich-like" structure known for other Ln(II) ions [91,93–98]. The complex $Eu(Tp^{Ph})_2$ (**4**) adopts an ideal trigonal antiprismatic (D_{3d} symmetry) molecular structure with a linear B–Eu–B fragment (Figure 1).

The D_{3d} single point group having C_3 axis is a subgroup of D_{6h}, which is enough effective to induce strong magnetic axiality in Ln complexes [99–102]. However, trigonal antiprismatic complexes of underexplored in the field of molecular magnetism. This is especially true for stable Ln^{2+} complexes of type **4**. However, one must take into account the grand state electronic configuration of the central ion when choosing a lanthanide for such studies. This is because the Ln^{2+} ions can have two electronic configurations: $4f^{n+1}5d^06s^0$ (for Nd, Sm, Eu, Dy, Tm, Yb) and $4f^n5d^16s^0$ (for La, Ce, Pr, Gd) [103]. The letters should be avoided in the design of new performant SIMs, due to the presence of an unpaired electron at the 5d level.

3.1.2. Complexes of tris(3,5-dimethylpyrazolyl)methane

The next group of tripods is a family of trispyrazolylmethane. In contrast to this boron congener tripod, tris(3,5-dimethylpyrazolyl)borate-anion, trispyrazolylmethane terdentate ligands are neutral in a majority known to date $[Ln(TPM)(anion)_3]$ (TPM = tris(3,5-dimethylpyrazolyl)methane) compounds. For the first time, air-stable complexes of rare earths with TPM were obtained in 2007 by Sella et al [45]. The six-coordinated complexes $[Ln(TPM)Cl_3](CH_3CN)_2$ were obtained in acetonitrile solution for Ln^{3+} = Y, Ce, Nd, Sm, Gd, and Yb. Authors have reported the crystal structure only for Y^{3+}. Later, Long et al [24] have studied isostructural complexes for Tb^{3+}, Dy^{3+} and Er^{3+} with the same composition. These compounds crystallize in the space group $P2_1/n$ with two solvent molecules. The molecular structure of $[Y(TPM)Cl_3](CH_3CN)_2$ (**5**) is presented in Figure 2. The SHAPE [104] analysis reveals that the coordination environment of Ln^{3+}-ion is a distorted octahedron in $[Ln(TPM)Cl_3](CH_3CN)_2$.

The isomorphous $[Ln(TPM)(OAr^{Me2})_3](thf)_3$ (**6**) (Ln = Y, Nd, Sm, Ar^{Me2} = Ph-2,6-Me_2) were obtained in a concentrated THF solution at −30 °C. These complexes crystallizes in the space group $P\bar{1}$ with three solvent molecules. The molecular structure of the $[Sm(TPM)(OAr^{Me2})_3](thf)_3$ (**6**) is shown in Figure 2. In all three compounds, each central ion is six coordinated with C_3 symmetry having the trigonal antiprismatic coordination environment of the metal center, with one smaller triangle composed of N-atoms and a larger one having OAr^{Me_2} groups in its vertices. This is seen clearly by comparing the ∠(N–Ln–N) and ∠(X–Ln–X) angles (~70 vs 100–108°). It should be noted, that in $[Ln(TPM)(OAr^{Me2})_3]$, the Ln–N distances (2.565(5) Å) are longer than those in **5** (2.459(5) Å), suggesting that the binding of the TPM tripod is subtle to modifications in steric demand of the adjacent ligands in the Ln coordination sphere. Compared with six-coordinate compounds comprising the isosteric but anionic Tp^{Me2} tripods, the average M–N distance is also noticeably longer (2.44(1) and 2.443(7) Å) in $[Sm(Tp^{Me2})]_2BPh_4$ and $[Sm(Tp^{Me2})_2]I$ [44], being consistent with the weaker Ln interaction of with neutral ligand.

Preprints (www.preprints.org) | NOT PEER-REVIEWED | Posted: 14 June 2023 doi:10.20944/preprints202306.0983.v1

5	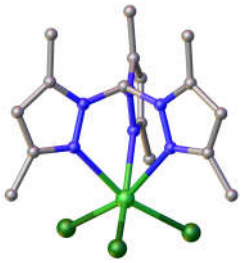	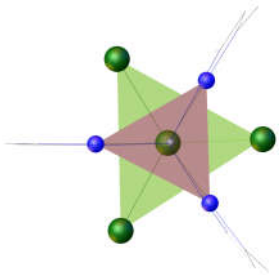
6	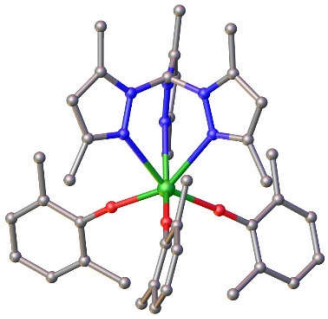	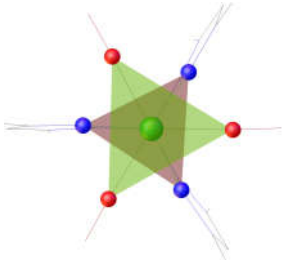
7	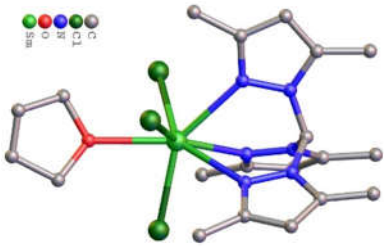	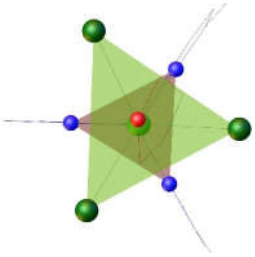
8	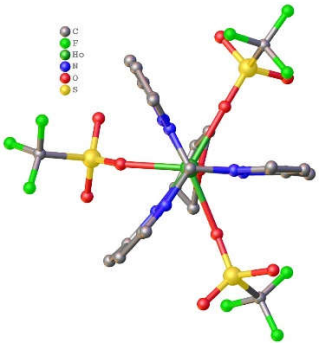	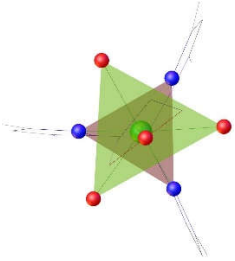
9	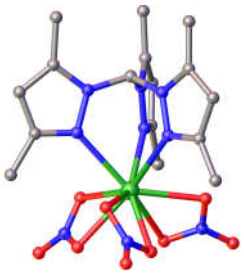	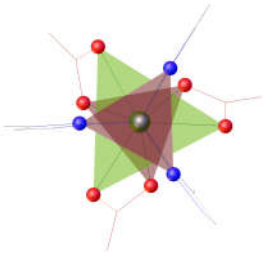
10	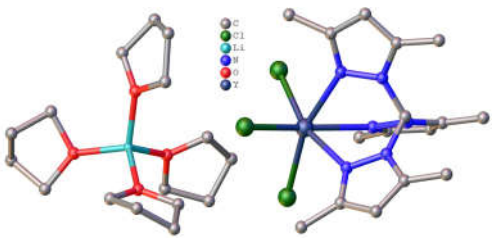	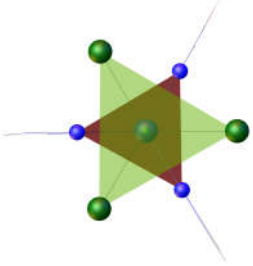

Preprints (www.preprints.org) | NOT PEER-REVIEWED | Posted: 14 June 2023 doi:10.20944/preprints202306.0983.v1

Figure 2. Molecular structures (left) and trigonal antiprismatic coordination polyhedra (right) for the compounds **5**-**10**. Hydrogen atoms are omitted. The picture was made using open crystallographic data.

The molecular structure of seven-coordinate [Sm(TPM)Cl_3(thf)]·thf (**7**) is presented in Figure 2. By contrast, with the unsolvated six-coordinate complex **5**, **7** contains one thf ligand, which can probably be accommodated due to larger coordination sphere of Sm than that of Y. The two studied [Ln(TPM)$(OTf)_3$(thf)] complexes are isomorphous due to the almost the same ionic radii of Y^{3+} and Ho^{3+}. The molecular structure of for the latter (**8**) is shown in Figure 2. The coordination sphere of the triflate or chloride complexes [Ln(TPM)$(X)_3$(thf)] may be described differently. Firstly, as a trigonal antiprism defined by one tripod and three anionic ligands (X = Cl, OTf), with a thf-ligand lying on the C_3 axis passing through the top of the tripod, and the triangular face defined by the anions. Secondly, as a tricapped trigonal pyramid, with the three N atoms of the TPM in the triangular base and with the thf oxygen defining the apex [45]. As in the case of the six-coordinate compounds, the triangles defined by the nitrogens are smaller than those defined by three anionic ligands.

Much later were synthesized and studied the three isomorphous complexes [Ln(TPM)$(NO_3)_3$]·MeCN (Ln^{3+} = Tb, Dy, Er), which crystallize in the $P2_1/n$ space group with one heteroleptic [Ln(TPM)$(NO_3)_3$] complex in the asymmetric unit [24]. The molecular structure of [Ln(TPM)$(NO_3)_3$]·MeCN (**9**) is presented in Figure 2. The coordination sphere of **9** is composed of three nitrogens from the tripodal ligand and six oxygens from bidentate nitrate anions. The Tb–N distances ranging from 2.482(2) to 2.530(2) Å are slightly longer than the Tb–O ones (2.416(2)–2.458(2) Å). The analysis of the 9-coordinate polyhedron by the SHAPE software indicates that the geometry of the lanthanide site could be best described as a spherical tricapped trigonal prism [24].

Magnetic studies for TPM coordination compounds were performed only for the two type of the anionic co-ligands (chloride and triflate) for the three Ln^{3+} ions - Tb, Dy, Er, congeners of the compounds **5** and **9**. For these complexes, the room temperature χT values correspond well to the theoretical ones predicted for single Ln ions consuming the free ion approximation. A temperature decrease induces a negative deviation of χT for all compounds, reflecting the depopulation of the m_J states [24]. Besides, the magnetization for the both series does not saturate even at a field of 7 T witnessing the pronounced magnetic anisotropy for all six complexes. Field induced slow magnetic relaxation was observed for all nitrate compounds and only for the Er congener of **5**. Based on these studies, the authors argue that the manifestation of a field-induced slow magnetization relaxation is greatly reliant on the anion's nature. While nitrate moieties appear to be suitable to stabilize the oblate electronic density of Dy^{3+}, chloride ions generate an equatorial crystal-field allowing the slow relaxation of the prolate Er^{3+} ions [24].

3.1.3. Complexes of anionic tripodal ligand − tris(3,5-dimethylpyrazolyl)-methanide

The electronic analog of tris(3,5-dimethylpyrazolyl)borate-anion is a deprotonated TPM − tris(3,5-dimethylpyrazolyl)-methanide (TPM*). Only a few Ln complexes are known to date [105]. Among them the three complexes with diamagnetic central Ln^{3+} ions [Ln(TPM*)Cl_3][Li(thf)$_4$] (Ln = Sc, Y (**10**), Lu) were synthesized and structurally characterized. The molecular structure of [Y(TPM*)Cl_3][Li(thf)$_4$] (**10**) is shown in Figure 2. All complex anions have C_3 symmetry, each metal ion being surrounded by three N atoms of the TPM* ligand and three chlorides, which form a distorted-octahedron polyhedron also found for **5**, despite the different space groups: $P2_1/n$ and R_3 for **5** and **10** respectively. It should be emphasized that the Y−N bond lengths of 2.425(5) Å for [Y(TPM*)Cl_3]$^-$ (in **10**) are somewhat shorter comparatively to those in the anions [Y(TPM)Cl_3]$^-$ and [Tb(TPM)Cl_3]$^-$ 2.459(2) Å [45] and 2.472(3)–2.490(3) Å [24]), but are closed to those of 2.425(6) Å for $DyCl_3(Tp^{Me_2})]^-$ [90]. This makes sense, since the tripodal ligand in both the latter and **10** has a negative charge, while the tripod in complexes with longer Ln-N bonds is neutral.

To our great regret, we could not find a single publication describing the magnetic properties of methanide-containing complexes of paramagnetic lanthanides.

Preprints (www.preprints.org) | NOT PEER-REVIEWED | Posted: 14 June 2023 doi:10.20944/preprints202306.0983.v1

3.2. Complexes with the pyridyl bearing tripodal ligand

Pyridine containing tripodal ligands have earlier been described [1]. Moreover, a diversity of bridgehead atoms such as nitrogen, carbon, and phosphorus [106], as well as other elements: Si [107], As [108], Al and In [109], Sn [110,111], Pb [112] and B [113] have been included to alter the properties of the coordination metal complexes both in terms of polyhedral geometry and to tune the electronic structure.

Strangely enough, structurally characterized complexes of the tris(2-pyridyl)methane class for lanthanides have not yet been obtained. Only a small group of exotic organometallic complexes based on tris(2-pyridyl)metallates that are unstable under normal conditions has been obtained and structurally characterized. This family of Ln-complexes will be briefly discussed in the next subparagraph of the review.

3.2.1. Complexes of tris(2-pyridyl)metallates

The most numerous group of Ln-complexes including tris(2-pyridyl)metallates are the coordination compounds of anionic tris(pyridyl)stannate (TPS) [114][115][116][117].

Interaction of [Ln(η^5-C_5Me_5)$_2$(OEt_2)] with the lithium [LiSn(2-Py-5-Me)$_3$(thf)] in THF solution using a 1:2 ratio gives the sandwich like [Ln{Sn(2-Py-5-Me)$_3$}$_2$] (**11**) complexes for divalent Ln = Eu and Yb [114]. The formation of **11** displays a more pronounced steric demand of the tripodal stannate ligand than C_5Me_5. This is comparable with similar reactions of tris(pyrazolyl)hydroborates $[HB(R_2pz)_3]^-$ (R = H, Me; pz = pyrazolyl) with [Ln(η^5-C_5Me_5)$_2$] species giving the analogous Ln^{II}-complexes [Ln($HB(R_2pz)_3$)$_2$] [114].

Both compounds **11** crystallize in the same space group $P2_12_12_1$ and have very close cell parameters. The molecular structure for europium complex is shown in Figure 3-11.

The Ln atoms of **11** are in a distorted octahedral coordination environment formed by six pyridyl nitrogens with a staggered organization of the pyridine rings around the Ln center. The coordination sphere around Ln is strongly distorted and the large size of the Ln atom affords a slight twisting of one of the pyridine rings of each Sn(2-Py-5-Me)$_3$ ligand unit around its Sn—C_{py} bond. Besides, the non-central location of the Ln atom in the cage is reflected by a bending of the Sn···Ln···Sn axis with 165.50(1)° and 167.28(13)° for Yb and Eu ions respectively [114]. The Sn bridgehead atom of the tripod reveals a trigonal pyramidal coordination mode (Figure 3-11, left).

The reaction of [LiSn(2-Py-5-Me)$_3$(thf)] with [Ln(η^5-C_5Me_5)$_2$] precursors resulted in formation of the first Ln^{II} sandwich complexes **12** involving the anionic TPS in a κ^3N-coordinating manner and featuring "naked" Sn^{II} centers, which can be used for following κ^1Sn-metal coordination (Eu complex is shown as example in Figure 3-12) [114].

Compound **12** crystallizes in the cubic space group $Pa\bar{3}$ with the Eu^{2+} lying on a special crystallographic position and four molecules in the unit cell. The longer Eu—N, (2.611(3) Å) and Eu···Sn (3.8874(4) Å) distances of are consistent with the larger size of the Eu^{2+} *vs* Yb^{2+} cation in **11**. The most pertinent feature is the Sn—Li contact of 2.792(12) Å in **12** is shorter than the covalent Sn—Li bond lengths (2.831–2.897 Å) [118]. Encapsulation of the large Eu^{2+} ion and additional κ^1Sn coordination of the two inner TPS ligands originates an opening of the tripodal structure (C-Sn-C = 99.6(1)°) compared to both outer TPS frameworks with "naked" Sn centers (C-Sn-C = 93.6(1)°) [114]. Furthermore, the κ^1Sn binding gives a practically ideal octahedral environment of the Eu^{2+} ion with a linear Sn···Eu···Sn axis (180.0(1)°).

1
1

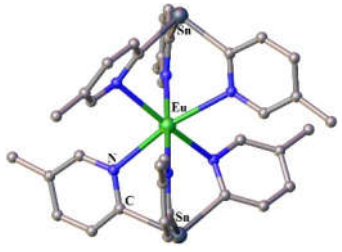

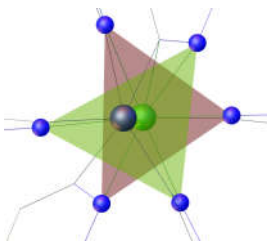

Preprints (www.preprints.org) | NOT PEER-REVIEWED | Posted: 14 June 2023 doi:10.20944/preprints202306.0983.v1

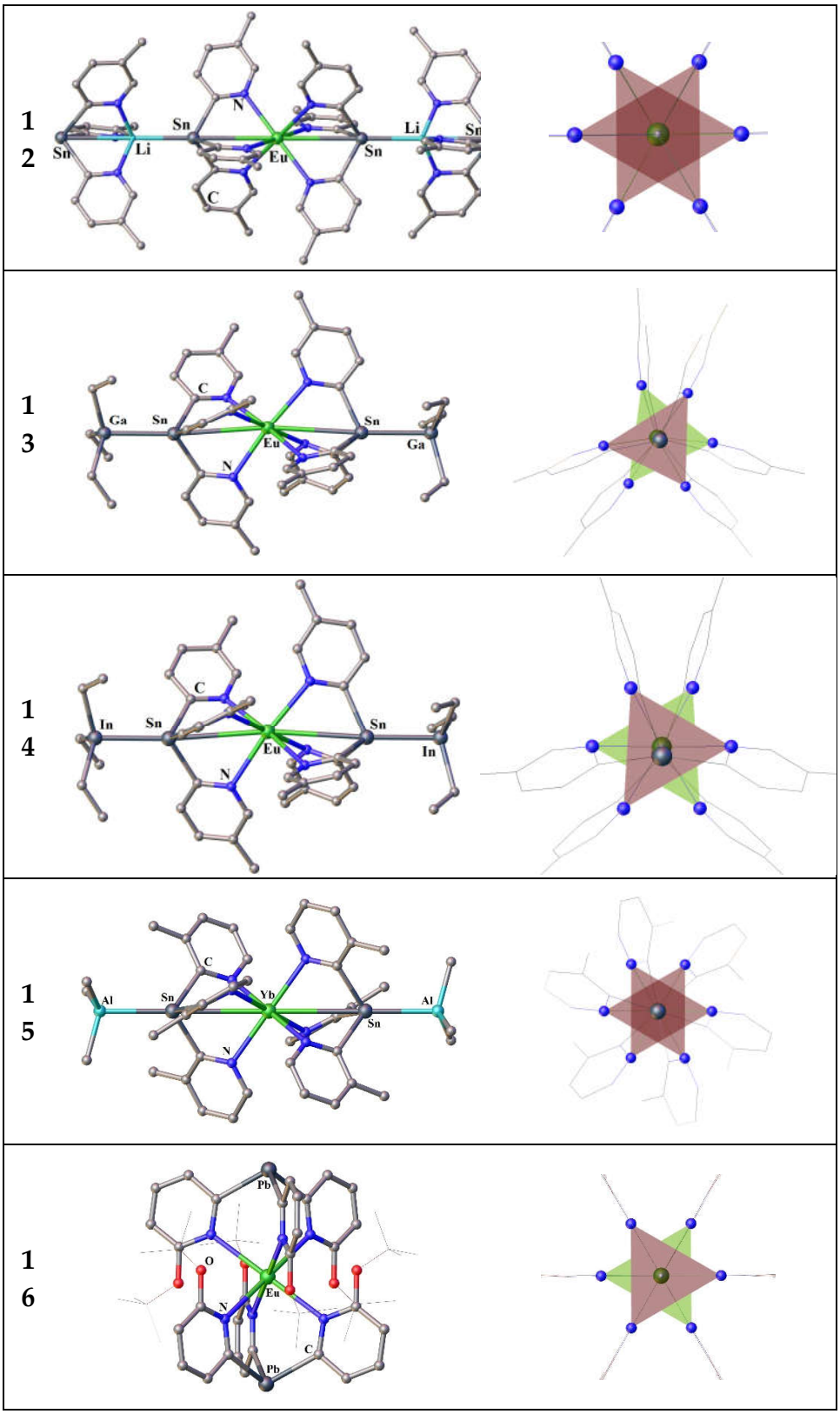

Figure 3. Molecular structures (left) and octahedral coordination polyhedra Ln-N_6, with colored faces forming the tripod bases (right) for the compounds **11**-**16**. Hydrogen atoms are omitted. The picture was made using open crystallographic data.

The room temperature reactions of a trialkylmetallates $MAlk_3$ (Alk = Me for Al, and Et for Ga and In) with complex [Ln{Sn(2-Py-n-Me)$_3$}$_2$] gave the following organometallic species: [Eu{Sn(2-Py-4-Me)$_3$}$_2${$GaEt_3$}$_2$] (**13**), Eu{Sn(2-Py-4-Me)$_3$}$_2${$InEt_3$}$_2$] (**14**) and [Yb{Sn(2-Py-3-Me)$_3$}$_2${$AlMe_3$}$_2$] (**15**) [115].

Preprints (www.preprints.org) | NOT PEER-REVIEWED | Posted: 14 June 2023 doi:10.20944/preprints202306.0983.v1

The compounds **13** and **14** (Figure 3) have the similar crystal structures crystallizing in the same space group *C2/c* [115], the Eu ions being in a distorted octahedral geometry, characteristic for the compounds **11** described above. In contrast with the complexes **11**, the non-central location of the Ln ion in the coordination octahedron **13** and **14** is much less expressed in the bending of the Sn···Eu···Sn axis by 176.40(5)° and 172.05(8)° for **13** and **14**, respectively. In the solid state, complex **15** (Figure 3) reveals bonding characteristics similar to those for **13** and **14**, but differs in that the Yb ion possesses almost perfect octahedral environment with a strictly linear Sn···Yb···Sn axis (180.0°) [115].

A few words about the only sandwich compound of a lanthanide complex comprising tris(2-pyridyl)plumbate. The compound [Eu{Pb(2-Py-6-O*t*Bu)$_3$}$_2$] (**16**) have been isolated from a concentrated THF solution [117]. Like **12**, the complex **16** (Figure 3) crystallized in *Pa*$\bar{3}$ space group. The Eu^{2+} ion is coordinated by six nitrogen donor atoms of two tripodal with Eu—N bond length of 2.699(2) Å Eu···O distance of 4.0215(1) Å, which is greater than those of 2.611(3) and 3.501(3) Å in **12**. This is because of a larger radius of bridgehead ion in Pb(2-Py-6-O*t*Bu)$_3$ tripod. Although the cavity of the tripodal ligand offers an almost ideal octahedral coordination sphere for the Eu^{2+} cation, which is well encapsulated and clearly separated from the formally negatively charged lead bridgehead atoms, compound **16** is not stable in THF solution [117].

The EPR solution studies at ambient conditions for **16** in presence of nitrosobenzene (NOB) suggested the generation of a radical entity. The X-band EPR spectrum exhibits one broad signal corresponding to a Eu^{II} $4f^7$ spin system with the value g_0=1.989±0.001 and a line width of ΔB_{PP}=(31.0±0.1) mT. An identical EPR spectrum was obtained and without spin trap. In addition to a broad signal, the spectrum shows a triplet of multiplets. The well-resolved hyperfine structure (hfs) is due to the coupling of the unpaired electron with the ^{14}N (I=1) nucleus and three groups of nonequivalent protons of NOB. The spectrum has been well simulated giving the values g_0=2.0057±0.0005 and a_0^N=(1.097±0.005) mT, as well as a_0^H=(0.249±0.005) mT, a_0^H=(0.235±0.005) mT, and a_0^H=(0.089±0.005) mT, respectively. The trapped radical was stable over a period of few hours. However, no ^{207}Pb hfs coupling could have been observed, indicating radical-adduct formation.

The complexes comprising tris(pyridyl)aluminate (TPAl) tripods are completed this section. As was shown by R. García-Rodríguez et al. [119,120], complexes of Ln^{2+} with TPAl are air unstable and can only be obtained employing sterically hindered tripods - [(Alkyl)Al(2-Py-6-R)$_3$]$^-$, where Alkyl = Et and R = Me or Br. It means that the coordination ability of TPAl can be adjusted by the steric and electronic character of substituents at a 6-position of the pyridyls. While [EtAl(2-py-6-Me)$_3$]$^-$ (**17**) coordinates strongly to Ln^{2+} ions, [EtAl(2-py-6-Br)$_3$]$^-$ (**18**) forms much weaker complexes, and [EtAl(2-py-6-CF$_3$)$_3$]$^-$ does not coordinate at all [120]. Synthetic and structural investigations were devoted essentially to the complexes of two anions [EtAl(2-Py-6-Me)$_3$]$^-$ and [EtAl(2-Py-6-Br)$_3$]$^-$. The 2 : 1 ratio reactions of the **17** with LnI$_2$ (Ln = Eu, Yb and Sm) in thf at room temperature gives deep-orange (Eu) or purple (Yb and Sm) solutions after 24 h, indicating of Ln coordination [119,120]. SC-XRD study confirmed a formation of the sandwich complexes: [{Ln(EtAl(2-py-6-Me)$_3$}$_2$] (Ln = Sm **18**, Eu **19**, Yb **20**) and [{Eu(EtAl(2-py-6-Br)$_3$}$_2$] (**21**), Figure 4. The complexes **18** and **21** crystallizes in *P* $\bar{1}$ space group. The first contains one $CH_3C_6H_5$ molecule as a solvate since it was crystalized from toluene. The coordination environment formed about the Sm and Eu are slightly elongated octahedron and trigonal antiprism respectively, although the both compounds have strait line passing through the bridgehead atoms of the tripods (Al-Ln-Al the angle is 180°). The compounds **19** and **20** crystallize in *P* 4_32_12 and *P* $2_1/n$ space groups correspondingly. Molecules of **19** and **20** feature six-coordinate, distorted-octahedral lanthanide metal ions with the N–Ln–N angles being approximately 90° and slightly bent Al–Ln–Al axis (177.17° (**19**) and 178.23° (**20**))[120].

Preprints (www.preprints.org) | NOT PEER-REVIEWED | Posted: 14 June 2023 doi:10.20944/preprints202306.0983.v1

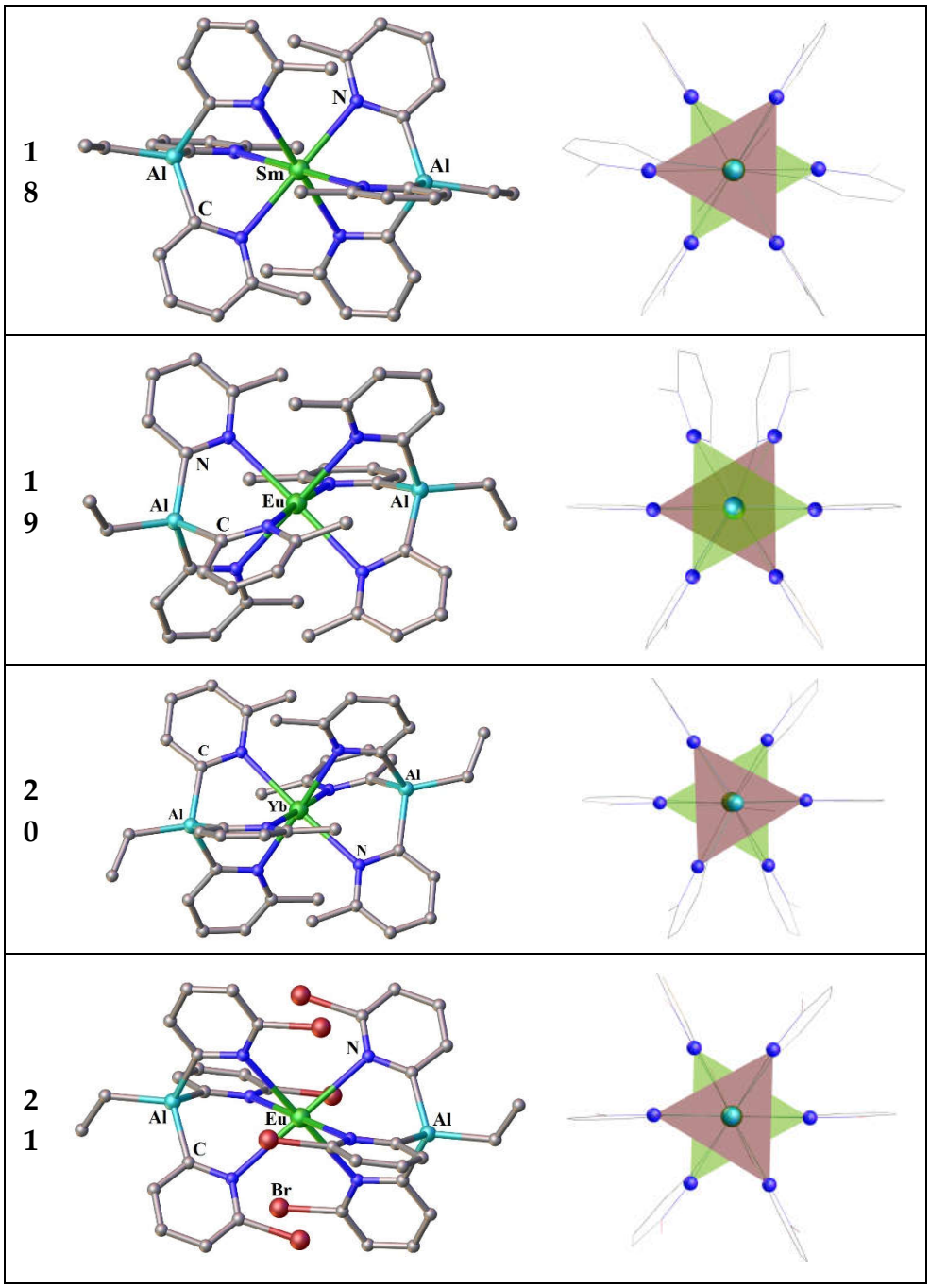

Figure 3. Molecular structures (left) and coordination polyhedra Ln-N_6, with colored faces forming the tripod bases (right) for the compounds **18**-**21**. Hydrogen atoms are omitted. The picture was made using open crystallographic data.

None of the Ln compounds comprising tris(2-pyridyl)metallates have been reported on their magnetic behavior. The next fairly representative group of lanthanide compounds with tripodal ligands are complexes with tris(2-pyridyl)amines.

3.2.2. Complexes of tris(2-pyridyl)amines

The interaction of tris(2-pyridylmethyl)amine (TPA) with the precursors $LnHal_3(thf)_4$ and $Ln(OTf)_3$ was investigated in anhydrous environment and in the presence of water [3,7]. In the absence of water, the succeeding formation of mono- and bis-(TPA) complexes were detected using Ln/ligand ratio of 1 and 2, respectively. The mono-TPA complexes $[Ce(TPA)I_3]$ (**22**) [3], $[Ln(TPA)Cl_3]$

Preprints (www.preprints.org) | NOT PEER-REVIEWED | Posted: 14 June 2023 doi:10.20944/preprints202306.0983.v1

(Ln(III) = Eu, Tb, Lu ([7]), and the bis(tpa) complexes $[Ln(TPA)_2]X_3$ (X = I, Ln^{3+} = La, Ce, Nd, Lu [3] and Sm [6]; X = OTf, bis(tpa) complexes

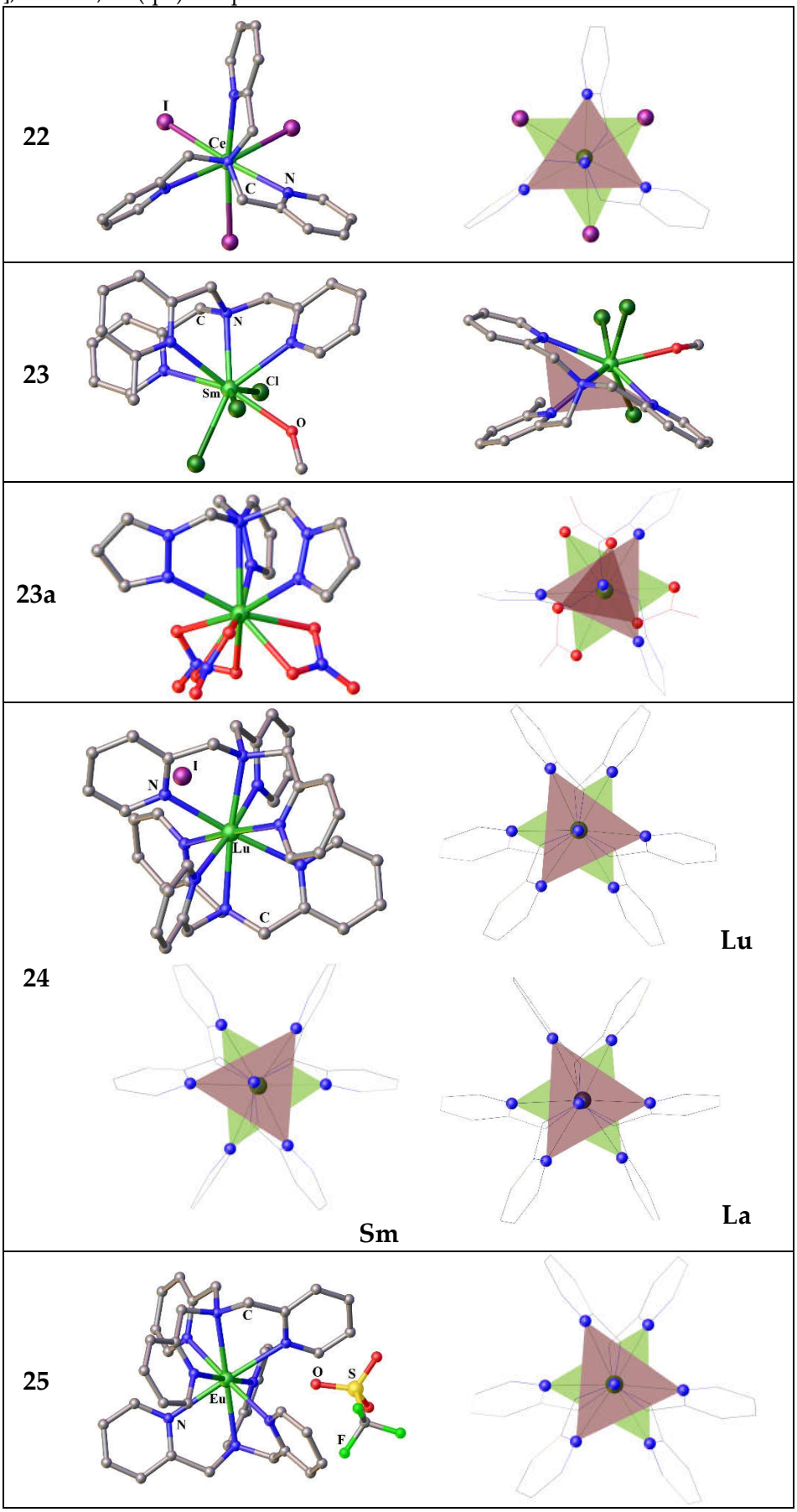

Preprints (www.preprints.org) | NOT PEER-REVIEWED | Posted: 14 June 2023 doi:10.20944/preprints202306.0983.v1

Figure 4. Molecular structures (left) and coordination polyhedra Ln-N_6, with colored faces forming the tripod bases (right) for the compounds **22**-**25**. Hydrogen atoms are omitted. The picture was made using open crystallographic data.

$[Ln(TPA)_2]X_3$ (X = I, Ln^{3+} = La, Ce, Nd, Lu [3] and Sm [6]; X = OTf, Eu [3]) were obtained under anhydrous conditions and their crystal structures were determined.

The complexes $[Ln(TPA)Hal_3]$ (see as example Figure 4-22) are isomorphous and crystalize in the space group $P2_1/c$ without any solvent molecules per a crystal cell. Note that the tripod base and a plane passing through the halide ions are not parallel.The mono-tripod complexes $[Ln(TPA)Cl_3(CH_3OH)]\cdot CH_3OH$ (**23**) (Ln^{3+} = La, Nd. Sm) (Figure 4) were also obtained starting from the corresponding hydrated lanthanide halide $[LnCl_3(H_2O)_6]$ [121]. Nonetheless, the compounds **23** are not of interest as high performance SMMs design because they do not have monoaxiality.

In contrast, a small group of heteroleptic complexes containing three nitrates and one tripodal tetradentate ligand tris((1*H*-pyrazol-1-yl)methyl)amine) (TPzMA) are enough axial, Figure 4-23a [12]. The authors present the synthesis, structures, and photophysical and magnetic properties of a sequence complexes $[Ln(TPzMA)(NO_3)_3]\cdot n$MeCN (Ln = Eu, Tb, Dy, Er, n = 0.5; Yb, n = 0). The SCXRD analysis reveals that, among the investigated compounds, the compounds of Eu, Tb, Dy, Er are isomorphous and crystallize in the triclinic $P\bar{1}$ space group with a single complex molecule and 1/2 of an CH_3CN molecule in the asymmetric unit. Their structures includes a mononuclear complex in which the Ln^{3+} ion coordinated by four N-atoms from TPzMA and six oxygens atoms belonging to three bidentate nitrate anions, Figure 4-23a. The tripodal ligand coordinates to the central ion in a symmetrical manner frowning together with nitrates the Ln^{3+} coordination polyhedron, which is better described as a distorted spherocorona [12]. Contrary to their congeners, the Yb complex crystallizes in the monoclinic $P2_1/c$ space group without solvates. Probably, due to the Ln contraction and the fall in intramolecular distances resulting in steric repulsions in the polyhedron, only two nitrate moieties are bidentate and the other one is monodentate, leading to a muffin geometry of the Yb site with Cs symmetry [12].

The europium, terbium, and dysprosium analogues exhibit a lanthanide-based luminescence, while the dysprosium, erbium, and ytterbium compounds show a field-induced slow relaxation of their magnetization involving Raman and direct processes.

The complexes $[Ln(TPA)_2]I_3\cdot CH_3CN$ (Ln = La, Ce, Nd, Sm) are isostructural to each other (see Figure 4-24) [3,6]. The metal ions are eight coordinate by the two-tetradentate ligands that wrap around the metal in a pseudo-D_3-symmetric arrangement [3]. All the complexes crystallize as a single enantiomer in the non-centrosymmetric space group $P2_12_12_1$ [3]. The coordination polyhedra are best defined as distorted cubes with a less distorted geometry for Lu [3].

It was not possible to obtain the crystal structure of $[Eu(TPA)_2]\cdot 3OTf$ under water-free conditions. The single crystals of $[Eu(TPA)_2]\cdot 3OTf\cdot CH_3CN\cdot 0.3H_2O$ (**25**) were obtained in the presence of ~0.5 equivalent of H_2O. The molecular structure of **25** (Figure 4-25) is very close to those of the Ln-bis(tpa) iodides. Contrarily to the complexes **24**, complex **25** crystallizes in a centro-symmetric space group $P\ 2_1/c$ with two complex molecules per asymmetric unit and 0.15 molecule of H_2O, which apparently helps the crystallization [3].

Along with to the Ln^{3+} TPA complexes, their congeners for Ln^{2+} were also isolated. Starting from LnI_2 the stable mono- and bis-TPA complexes: $[Yb(TPA)I_2(MeCN)]\cdot$MeCN (**26**, Figure 5-26) and $[Ln(TPA)I_2]$ (Ln^{2+} = Sm, Eu) (**27**), $[Ln(TPA)_2]\cdot 2I\cdot 0.5$MeCM ($Ln^{2+}$ = Sm, Yb) (**28**, Figure 5-28) were prepared and characterized [6]. When a bulk anion $NaBPh_4$ is added to the previous reaction mixture, a number of compounds with TPA and its analogs methylated, a family of Ln^{2+} complexes was also obtained in inert conditions [122]. The compounds $[Ln(Me_nTPA)_2](BPh_4)_2$ (n = 0–3 reliant to methylation degree of the 6-position of the pyridyl rings of Me_nTPA, when n = 0 — Ln^{2+} = Eu, Yb **29** (Figure 5-29), n = 2 — Ln^{2+} = Eu, Yb (**30**) and n = 3 — Ln^{2+} = Eu (**31**, Figure 5-31)) have been synthesized and their structural, electrochemical and photophysical properties studied [122].

Preprints (www.preprints.org) | NOT PEER-REVIEWED | Posted: 14 June 2023 doi:10.20944/preprints202306.0983.v1

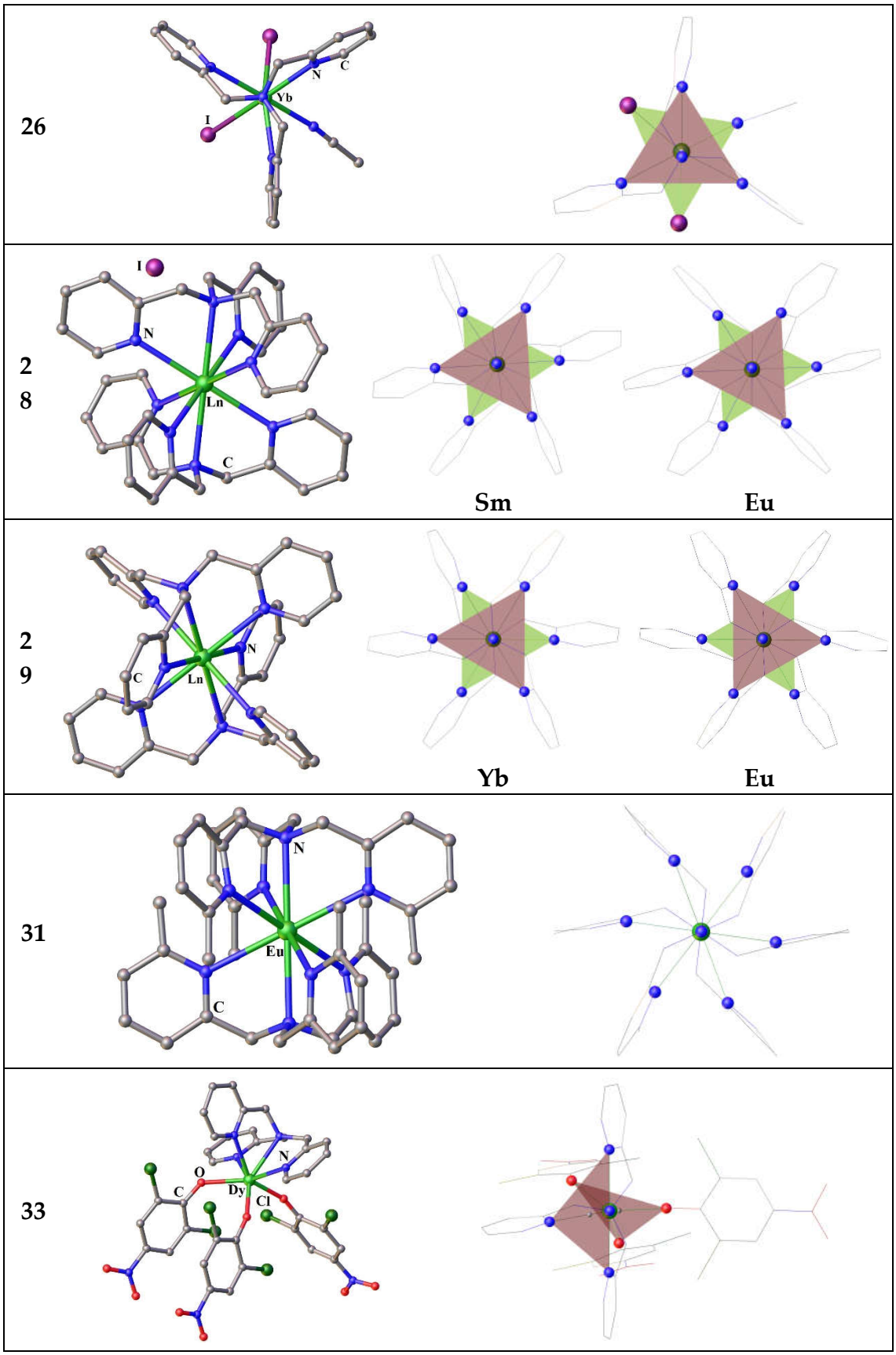

Figure 5. Molecular structures (left) and coordination polyhedra Ln-N_6, with colored faces forming the tripod bases (right) for the compounds **26**-**33**. Hydrogen atoms are omitted. The picture was made using open crystallographic data.

Preprints (www.preprints.org) | NOT PEER-REVIEWED | Posted: 14 June 2023 doi:10.20944/preprints202306.0983.v1

The complexes **27**, $[Ln(TPA)_2]\cdot 2I$, crystallize in the monoclinic centrosymmetric $P2_1/c$ space group while the complexes **28**, $[Ln(TPA)_2]\cdot 2I\cdot 0.5CH_3CN$ crystallize in the non-centrosymmetric monoclinic Cc space group [6].

Complexes **29** crystallize in the monoclinic $P2_1/n$ space group, contrary to **30** and **31**, which crystallize in the triclinic $P1^-$ space group, with the lowering of symmetry attributed to the presence of the methyl substituents that result in crystallographic disorder [122]. The Ln^{2+} ion is 8-coordinate in all sandwich compounds. Continuous shape measures using the software SHAPE 2.1 were employed to determine the geometry of the Ln centers and suggest that the coordination geometry is closest to cubic in all cases [122]. The Shape distortion parameters are in the range 0.69–1.53 for the cubic geometry, the further the value being from zero, the greater the distortion from ideal geometry [122].

Unfortunately, for all the above compounds comprising TPA (both for sandwich and semisandwich), the magnetic properties have not been studied. Only two $[Ln(TPA)(Anion)_3]$ compounds and four $[Ln(TPzMA)(NO_3)_3]\cdot$complexes have been magnetically characterized [123]. The description of their magnetic behavior we conclude the current section of the review.

Two mononuclear seven-coordinate Dy^{3+} complexes $[Dy(TPA)Cl_3]$ (**32**) and $[Dy(TPA)(OPhCl_2NO_2)_3]\cdot 0.5CH_2Cl_2$ (**33**) have been synthesized based on the neutral ligand TPA and either the strong strength ligand 2,6-dichloro-4-nitrophenol (Cl_2NO_2PhOH) or the weak ligand field donor Cl^- [123]. As in the tri-iodine compounds of type **22**, mentioned above, the Dy^{3+} ions in complexes **32** and **33** have seven-coordinated capped octahedral and capped trigonal prismatic coordination geometries, respectively [123]. Magnetic studies showed that both Dy compounds possess field-induced slow magnetic relaxation. The energy barrier for **33** is higher than that of **32**, which is due to the strong ligand field of $Cl_2NO_2PhO^-$*versus* Cl^-, resulting in a larger magnetic anisotropy of **33** as compared to **32** [123]. The direction of the magnetic anisotropy axes in both complexes deviate remarkably from the symmetry axis of the capped octahedron (C_{3v}) and the capped trigonal prismatic (C_{2v}), which explains the poor performance of SIM behavior for both complexes [123].

The room-temperature χT values of 12.97, 13.92, 11.54, and 3.20 emu/mol for **23a**, respectively for $[Ln(TPzMA)(NO_3)_3]\cdot$(Ln = Tb, Dy, Er, Yb), are in quite good accordance with the theoretical values of 11.82, 14.17, 11.48, and 2.57 emu/mol estimated for a unique Ln^{3+} ion [12]. Upon cooling, all compounds exhibit the typical decrease in χT caused by the thermal depopulation of the m_J levels reaching values at 1.8 K of 5.25, 7.35 [12]. For all complexes, the absence of saturation for the magnetization curves testifies to the existence of magnetic anisotropy, as expected for such lanthanide ions [12]. Under a zero-dc field, no strong out-of-phase susceptibility (χ'') components was observed for any of the samples pointing out the occurrence of fast QTM.

Excluding the Tb complex, for which the out-of-phase component remains weak, all other complexes show a strong χ'' component upon applying *dc* field. For the Er and Yb compounds, the appearance of a second low-frequency peak was detected at high magnetic fields. It might originate from different relaxation mechanisms actuated by large magnetic fields [12]. Appears therefore that the neutral tetradentate TPzMA ligand in association with nitrates and the resulting low-symmetry of the lanthanide site do not provide the requirements to maximize the anisotropy for either oblate or prolate lanthanide ions in zero dc field [12].

4.1. Complexes of the tripodal nitroxyl radicals

Metal-radical systems are recognized to display better SMM characteristics [124]. For example, an extra electron transforms $(n\text{-}Bu)_4N[TbPc_2]$ (Pc is a dianion of phthalocyanine) into $[TbPc_2]$ (Kramers system), guaranteeing twofold degeneracy of all electronic levels enforced by time reversal symmetry, irrespective to ligand field symmetry[125]. Park et al. [126] stated that the higher energy levels sturdily depend on the ligand type, molecular symmetry, and overall charge of the molecules. Additionally, ligand distortion and molecular symmetry play a key role in transverse CF parameters leading to tunnel splitting. The latter induces QTM. Compared to the anionic complex $[TbPc_2]^-$, for the neutral complex, no tunnel splitting was observed for the ground and excited state quasi-doublets

Preprints (www.preprints.org) | NOT PEER-REVIEWED | Posted: 14 June 2023 doi:10.20944/preprints202306.0983.v1

[126]. For the anionic complex, the tunnel splittings of 0.007, 0.090, and 7.969 cm^{-1} have been observed for the ground, first and second excited state quasi doublets. The perceived dissimilarity in the magnetic behavior was attributed to the significant an exchange interaction, J_{ex} of ~ 7 cm^{-1}, existing in the compound [$TbPc_2$] compared to the anionic one [126]. Moreover, the axial CF parameter (B_2^0 = –5.93 *vs* –5.05 cm^{-1}) is larger, and the transverse CF parameter (B_2^2 = 0.3 to 0.4 cm^{-1} vs. 0.8 to 3.6 cm^{-1}) is small for the latter [126].

Real influence of exchange coupling on magnetic relaxation dynamics was reported by Long et al., firstly reported very large T_B values [127]. They have obtained the binuclear Tb^{3+} complex [{[$(Me_3Si)_2N]_2(THF)Tb\}_2(\mu$-$\eta^2$:$\eta^2$-$N_2)^-$] (**$TbN_2Tb$**), in which the large magnetic interaction between Tb^{3+} and radical established to quench QTM in the absence of magnetic field. This SMM relaxes in the thermally activated direct process having (QTM probability B~10^{-6}) an U_{eff}=227 cm^{-1} and T_B~14 K [127]. Later, the strong coupling of –27 cm^{-1} was communicated for the Gd congener of **TbN_2Tb** [128]. For the **GdN_2Gd** the electronic structure calculations have been performed, which clearly evidence about the direct overlap between the Gd^{3+} 4f-orbitals and the π^* orbital of the radical [129].

4.1.1. The functionalized by 2-pyridyl groups paramagnetic tripods and their complexes

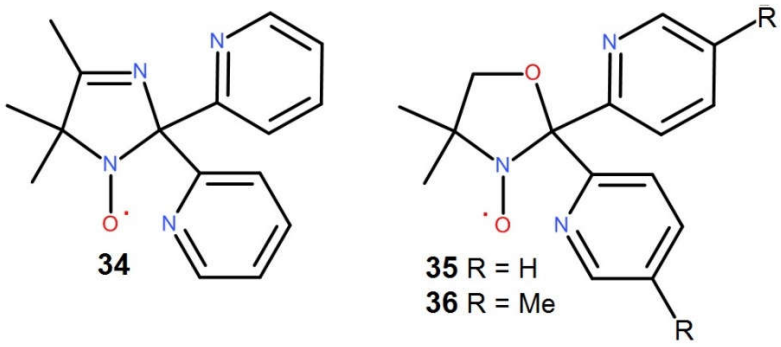

Figure 6. 2,5-Dihydro-4,5,5-Trimethyl-2,2-Bis(2-Pyridyl)Imidazole-1-Oxyl. **34**; 4,4-dimethyl-2,2-di(2-pyridyl) oxazolidine-N-oxyl **35** and 4,4-dimethyl-2,2-bis[2-(4-methylpyridyl)]oxazolidine-N-oxyl **36** – radical tripods.

Nitroxyl stable radicals a widely used in the field of molecular magnetism [130–135]. However, till now only three tripodal nitroxyl radical functionalized by pyridyl groups (Figure 6) are known [25,136]. The complexes of the 3d metal ions with the radical tripods **34-36** are most of a sandwich type [25–32,137]), while a number of semi-sandwich Ln-complexes were recently synthesized [138,139] (Figure 7-37). In contrast to the tetradentate tripods of TPA described above, the tripodal oxazolidine radical (Rad) **35** is sterically rigid, forming a pyramid upon coordination with an almost right triangle at the face for both monoradical (**37**) and biradical complexes (**38**) (Figure 7) [138,140].

4.1.2. Structural features of the paramagnetic tripod complexes

According to PRXD study, the monoradical complexes [$LnRad(NO_3)_3$] (**37**) are isostructural. The crystal structures for the **37** complexes of Ln^{3+} = Dy, Tm, Y, Eu and Lu ascertained by SC-RXD experiments. Like their closest relatives, the nitrate complexes of Ln with diamagnetic tripod TPM (**9**), the compounds **37** crystallize in the non-centro symmetric $P2_1/n$ space group [138]. In this complexes, Rad coordinates the Ln ion in a tridentate manner via two N atoms of the pyridyl substituents and an O atom of an NO group. The coordination sphere is further complemented by three bidentate nitrates to give an LnO_7N_2 polyhedron [138]. Consistent with the continuous symmetry measures method [104], the polyhedron is best described as a spherical tricapped trigonal prism. The radical donor atoms compose a triangular face of the prism. In addition, the coordinated oxygen atoms of the nitrate ligands, they also form triangular planes parallel to that of Rad (Figure 7-37, right). Moreover, the centers of all triangles lie on the same axis passing through the central Ln atom, which bears witness to with S_3 symmetry.

Preprints (www.preprints.org) | NOT PEER-REVIEWED | Posted: 14 June 2023 doi:10.20944/preprints202306.0983.v1

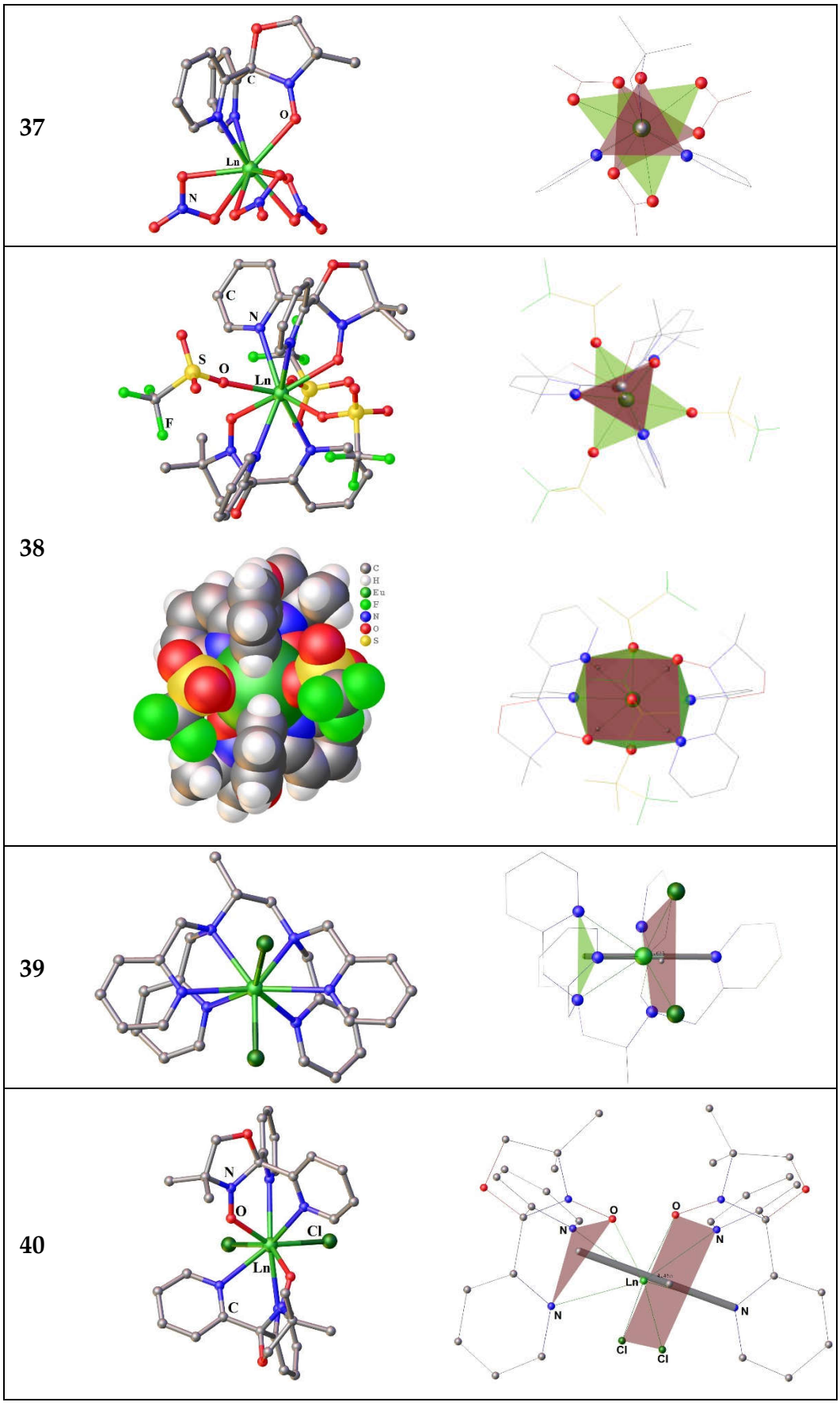

Figure 7. Molecular structures (left) and coordination Ln polyhedra with colored triangles forming the tripod bases (right) for the compounds **37**-**39**. Hydrogen atoms are omitted. The picture was made using open crystallographic data.

Preprints (www.preprints.org) | NOT PEER-REVIEWED | Posted: 14 June 2023 doi:10.20944/preprints202306.0983.v1

The Ln–O bond distances related to the NO moiety vary in region of 2.34 – 2.38 Å. N – O bonds length of the nitroxyl group fluctuate in the 1.25–1.28 Å interval. Markedly, all bond lengths and angles of the complexes are in the expected range [138]. In biradical complexes **38**, the mode of ligand coordination does not differ from that of monoradical complexes **37**. The Ln environment is composed of three monodentate anions to give LnO_5N_4 polyhedron. Unlike nitrate ligands, triflates are bound to Ln by only one donor O atom and are located in the equatorial plane of the compounds **38**. At first glance, the latter have D_{3h} pseudosymmetry, since both tripod bases are placed one above the other, and the donor atoms of the OTf ligands form a triangle (Figure 7-38). However, due to the "sandwich" bending, all triangles are highly distorted. Though, the SHAPE analysis [104] gave the polyhedron geometry as a spherical capped square antiprism with the point symmetry close to C_{4v} [140]. The radical donor atoms and two OTf compose faces of the antiprism while oxygen of the third triflate arranges above the rectangular face [140].

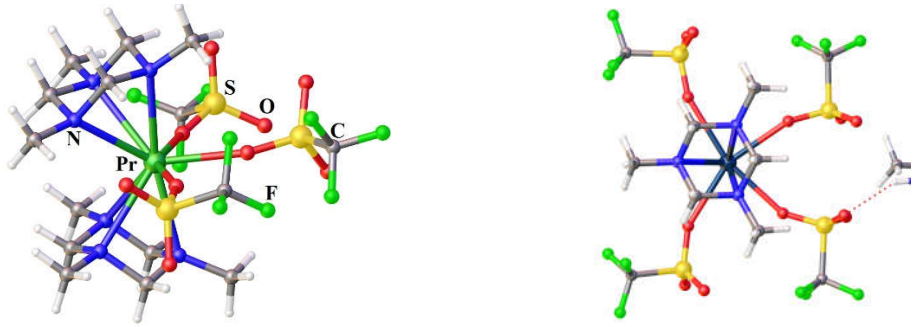

(**a**) (**b**)

Figure 8. (a) Tri-triflate $[Pr(Me_3tach)_2(OTf)_3]$ [141]; (**b**) Four-triflate $HMe_3tach[La(Me_3tach)_2(OTf)_4]$ [142] complexes. The picture was made using open crystallographic data.

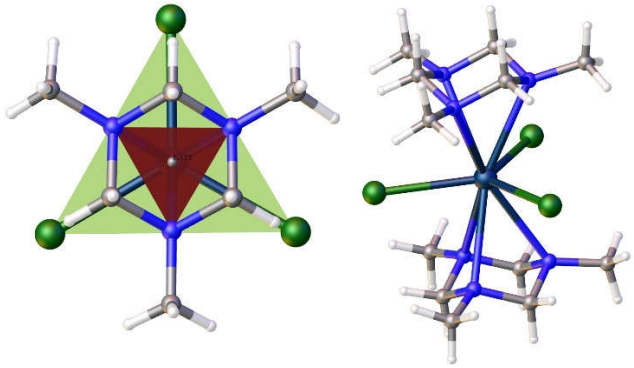

Figure 9. The compound $[La(Me_3tach)_2Cl_3]$ having three chlorine anionic ligands in equatorial plane.

Only two related compounds for the sandwich complex **38** are Ln^{3+} complexes with a quasi tripodal ligand 1,3,5-trimethyl-triazacyclohexane (Me_3tach) – $[Pr(Me_3tach)_2(OTf)_3]$ [141] and $HMe_3tach[La(Me_3tach)_2(OTf)_4]$ [142], Figure 8. The first is so bent that the three triflates are not evenly distributed in the equatorial plane, while the latter is capable to house even more triflates. Such a geometrical organization of the Ln coordination sphere is favorable to stabilize the highest m_J ground states for the prolate tripositive lanthanides ions (Pm, Sm, Er, Tm, and Yb). That is why the **38**-Dy complex studied by us earlier does not exhibit slow magnetic relaxation. The most attractive geometry (for prolate type Ln^{3+}) among compounds with this pseudotripodal ligand has the recently studied the only non-bent sandwich complex $[La(Me_3tach)_2Cl_3]$ [142] having three chlorine anionic ligands in equatorial plane, Figure 9. However, chloride anions are bulky enough to enter threesome the inner sphere of smaller Ln^{3+} ion beginning from samarium. Nevertheless, two chlorides can fit quite well in the equatorial plane of the Ln coordination sphere. We did not find an example of such a specie for any $[Ln(tripod)_2Cl_2]^+$. According to the CCDC, there are only a few examples of such compounds with bis-tripodal ligands. One of which is the Eu^{3+} complex $[Eu^{III}Cl_2\{R)\text{-tppn}\}]ClO_4$ (**39**)

Preprints (www.preprints.org) | NOT PEER-REVIEWED | Posted: 14 June 2023 doi:10.20944/preprints202306.0983.v1

[143], Figure 7. The coordination geometry of **39** is best described as a distorted dodecahedron. The authors point out that the four coordinated pyridyl nitrogens and one from the two Cl-atoms are approximately on a plane and form a pentagon, the other Cl being coordinated almost perpendicular to this plane. However, from our point of view, it is better to choose a different description of the geometry of the compound **39** in order to predict the magnetic behavior. Both Cl anions are best placed in the same plane, as shown in Figure 8. In this case, the molecule have an axis, which could serve as an axis of anisotropy. Our preliminary studies have shown that sandwich-type complexes containing two chloride ligands in the equatorial plane of the cationic complex **40** (Figure 7) can also be obtained for the paramagnetic tripod **35** [144].

4.1.3. Magnetic properties of the paramagnetic tripod complexes

At 300 K, the χT product values are 7.814, 12.210, 14.366, 7.376 emu K/mol for the **37** type compounds of Gd, Tb, Dy, and Tm, respectively. These values are well consistent with the expected ones for the appropriate Ln^{III} ion plus a radical (8.255, 12.195, 14.545, 7.525 emu K/mol) [138]. With the temperature lowering, the χT value for all derivatives drops considerably, which can be ascribed to CFS and/or the antiferromagnetic metal-radical interaction. It could be assumed a dominance of the CFS for all Ln except Gd, which is magnetically isotropic at first order. It should be emphasized, that the **37-Tm** complex, for which the nonmagnetic $m_J = 0$ ground state is stabilized (χT is equal to 0.375 emu K/mol corresponding to the value of a radical tripod). Furthermore, the important decrease in χT for **37-Gd** bears witness to a strong antiferromagnetic (AFM) coupling between the Gd^{III} ion and the radical. The plot M(H) for the **37-Gd** complex is very informative. Considering the low crystal field splitting typical of Gd^{3+}, the saturation value of 6 μ_B is consistent with an AFM coupling between a spin $S = 7/2$ and a radical spin $S = ½$ ($S_{tot} = 7/2\text{-}1/2 = 3$) [138]. X band EPR has been performed on $[GdRad(NO_3)_3]$ in order to obtain precise information about the electronic structure. The spectrum of Gd exhibits several broad transitions.

A satisfactory fitting of both the EPR and the static magnetic measurements can be obtained using the following Hamiltonian:

$$\mathcal{H} = b_2^0\hat{O}_2^0 + b_2^2\hat{O}_2^2 + b_4^0\hat{O}_4^0 + j\hat{S}_{Gd}\cdot\hat{S}_{rad} + g_{Gd}\mu_B\hat{S}_{Gd}\cdot B + g_{rad}\mu_B\hat{S}_{rad}\cdot B \text{ [138]} \quad (1)$$

where the first three terms parametrize the CFS of the Gd^{III} ion, the fourth term is the isotropic magnetic coupling between Gd and the radical and the last two terms are the Zeeman splitting for Gd and the radical, respectively. The finest simulation result was achieved with the values $b_2^0 = 5.2\ 10^{-2}$ cm^{-1}, $b_2^2 = 1.1\ 10^{-2}$ cm^{-1}, $b_4^0 = 3.8\ 10^{-4}$ cm^{-1}, $j = +23$ cm^{-1}, $g_{Gd} = 2.0023$ and $g_{rad} = 1.998$. Notably, the value of +23 cm^{-1} of the isotropic coupling constant is unusually large for gadolinium complexes of organic radicals. For example, for Gd^{3+} hexafluoroacetylacetonate complexes containing one acyclic nitroxyl radical [145–147] the $|j|$ value of fluctuates between 9.6 and 12.5 cm^{-1}. For the similar compounds including one nitronyl nitroxyl radical [148–153], exchange coupling is also inferior ($|j| = 0.77 \div 8.35$ cm^{-1}). For the Gd-complex comprising congener of Rad TEMPO (TEMPO = 2,2,6,6-tetramethylpiperidin-1-oxyl) metal-radical interaction is very small ($j = 2.43$ cm^{-1}) [154]. For the mono-semiquinone complex $[Gd(HBTp_3)_2SQ]$ $j = 11.4$ cm^{-1} [155]. Moreover, the exchange interaction strength for Gd-radical in the $[GdRad(NO_3)_3]$ species is comparable with for the binuclear Gd complex of the purely inorganic single radical N_2^{3-} obtained in the group of Long [128]. The origin of such a strong magnetic exchange interaction in **37** must be ascribed to a favorable metal-to-ligand orbital superposition. In contrast to the most studied complexes with nitronyl and imino-nitroxyl radicals, in which the spin density is mainly delocalized over four or three centers (O - N ... N – O [156], N ... N - O), in **37**, an unpaired electron is shared by only two cites. Consequently, the spin density on the donor oxygen atom in Rad is two times higher than that in the nitronyl nitroxyl radical. Notably, the exchange interaction is directly related to magnetic orbital overlapping, which depends on the symmetry and donor strength of all ligands [138].

Dynamic magnetic studies were to get information on the magnetization dynamics at low temperatures. A frequency scan at various applied fields for **37** was performed at the temperature of 2 K. The only compound to display a relevant nonzero out of phase magnetic susceptibilities was **37-**

Preprints (www.preprints.org) | NOT PEER-REVIEWED | Posted: 14 June 2023 doi:10.20944/preprints202306.0983.v1

Tb. The latter displays slow relaxation both with and without an external applied field. In zero applied field the relaxation of **37-Tb** at 2 K is at the upper edge of accessible frequencies with relaxation time ca. 16 μs, for this reason a temperature study was impossible. When an external magnetic field was applied, the slow relaxation of **37-Tb** slows by several orders of magnitude [138]. The relaxation time best fit was obtained using a combination of quantum tunnelling and Orbach processes, giving τ_{QT}=12(1) ms, τ_0 = 0.9(3) ns and ΔE = 57 cm^{-1} [138].

The magnetic studies on powder samples of the complexes **38** were also fulfilled. The $\chi_m T$-value at 300 K for the **38-Dy** compound (14.735 emu K/mol) is slightly smaller than theoretical one (14.92 emu K/mol) for the non-interacting two radicals and one Dy^{3+} ion (S = 1/2, g = 2.0023, 0.375 emu K/mol) ($4f^9$, S = 5/2, L = 5, J = 15/2, g_J = 4/3, $^6H_{15/2}$, 14.17 emu K/mol). However, this value corresponds well to those of 14.365 emu K /mol, previously obtained for the monoradical complex 37-Dy [138] taking into account the fact that the experimental values for Dy^{3+} in a related coordination environment are somewhat lower than those for a free ion: 13.92–14.00 [12,157]. On cooling, the $\chi_m T$ value remains almost unchanged up to 90 K, and then steadily falls down to 10 emu K mol^{-1} at 20 K and finely drops to 4.803 emu K mol^{-1} at 2 K. The latter is considerably lower than that for the monoradical analogue (6.50 emu K/mol). Since significant intermolecular exchange interactions in **38-Dy** can be excluded, the cause of such behavior could be attributed to the radical-radical coupling, which can reach high values ($J_{TEMPO1\text{-}TEMPO2}/k_B$ = −24.9 K) in [Y(hfac)$_3$(TEMPO)$_2$]) [158]. Moreover, the metal-to-radical coupling in the [Gd(hfac)$_3$(TEMPO)$_2$] has been reported to be either positive or negative for the different radicals of the same molecule ($J_{Gd\text{–}TEMPO}/k_B$ = −6.45 and +4.0 K, obscuring the picture [158]. Therefore, for the very anisotropic Dy, it is difficult to obtain more information also due to the high mixing of the $|J,m_J>$ levels favored by the relatively low-symmetry ligand field. In order to elucidate the nature of exchange interactions in **38-Dy** [158].

The temperature dependence of $\chi_m T$ for Eu^{3+} compounds is determined by the thermal population of the $^7F_1$ level nearest to the ground nonmagnetic level $^7F_0$. The excited $^7F_1$ state, closely sited to the ground one, is partly populated already at room temperature. At 300 K, $\chi_m T$ for Eu^{3+} complexes with diamagnetic organic ligands can vary in the range of 1.032–1.386 emu K/mol[1] depending on the ligand field parameters [159]. Therefore, for the complex **38-Eu**, the 300 K $\chi_m T$ value of 1.778 emu K/mol is reasonable for the two uncoupled radicals and one Eu^{3+} ion, but lower than the value of 1.93 emu K/mol found for the bis-nitronylnitroxide (NN) complex [Eu(NN)$_2$(NO$_3$)$_3$] with a different coordination environment (N_{10} instead of N_4O_5) [160]. As the temperature pulls down, the $\chi_m T$ decreases gradually, and, starting from 9 K, drops to 0.348 emu K/mol, which is somewhat higher than that for [Eu(NN)$_2$(NO$_3$)$_3$] compound (0.24 emu K/mol). No ac signal was observed in either sample in the measurable interval of frequencies (0.1–10,000 Hz).

4.1.4. Rational design of the paramagnetic tripods and their complexes

As mentioned above, in the presence of anionic ligands in the equatorial plane, it is better to use prolate Ln ions: Pm, Sm, Er, Tm, and Yb. While for more "magnetic" dysprosium and terbium, the presence of anionic ligands at the equator is strictly contraindicated. Therefore, it is necessary to change the structure of the paramagnetic tripod so that there is no space for anionic ligands or solvent molecules in the Ln coordination sphere. An analysis of the molecular structure of sandwich complexes with diamagnetic tripods has showed that low-coordination compounds without anionic ligands are formed in the presence of steric hindrance in a position adjacent to donor tripod atoms giving propeller-like structures with ideal axiality (see compounds **1**, **4**, **16**, **18**, **21**, **31**). It should be noted that in most of the bis-tripodal complexes considered in this review, the ligands are symmetrical tripods, in contrast to the radical **35**, which consists of two six- and one five-membered heterocycles. Moreover, the latter comprises a bridgehead carbon atom in ligand. While, other described tripods are more spatial ligands. In complexes with the radical **35**, the average value for the side length of the triangular base is about 2.8 Å, while for other bridgeheads it is much larger: 2.9-3.1 for boron, 3.8-4.0 for nitrogen and metallic bridgehead. The larger dimensions allow to the tripods with hetero bridgehead atom “to more deeply set on the head” of the central Ln ion.

Preprints (www.preprints.org) | NOT PEER-REVIEWED | Posted: 14 June 2023 doi:10.20944/preprints202306.0983.v1

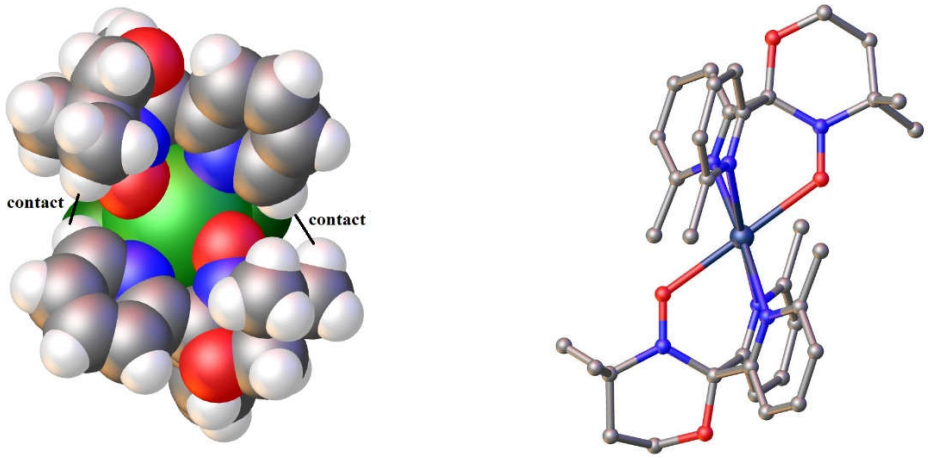

(**a**) (**b**)

Figure 10. (a) The closest contacts in $[DyRad_2Cl_2]^+$; **(b)** Bis-(oxazinane-radical) Ln complex cation.

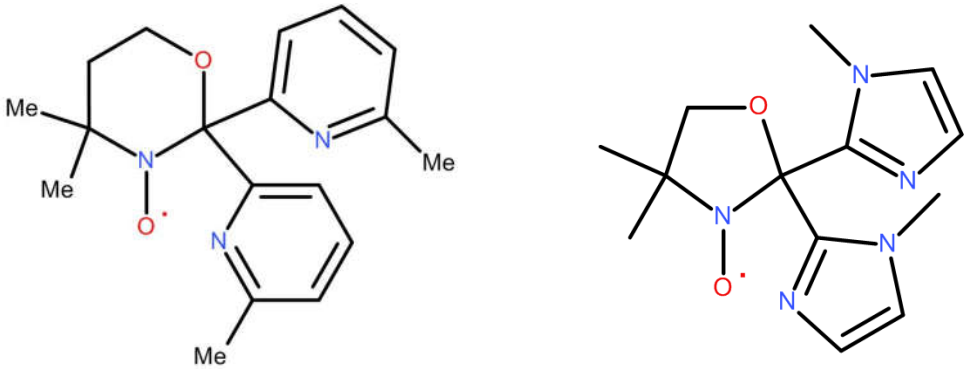

(**a**) (**b**)

Figure 11. More sterically demanding and more symmetrical candidates as tripodal nitroxyl radicals: (**a**) 4,4-dimethyl-2,2-bis[2-(3-methylpyridyl)]oxazinane-N-oxyl (**41**); (**b**) 2,2-bis[2-(1-methyl-imidazol-2-yl)]oxazolidine-N-oxyl (**42**).

On the space filling image of the "burger" **38** (Figure 7), it is clearly seen that two pyridyl substituents of the different oxazolidine radicals **35** are in close proximity, and the shortest contact H…H between them is equal to 2.41 Å. In complex **40**, there are also sufficiently close distances between the pyridine rings and the methyl groups of the radical (2.613 and 3.007 Å, Figure 10). Therefore, if an additional methyl group is located in the fourth position of the pyridyl rings (just near donor nitrogen atom), then most likely this will be enough for the paramagnetic tripods to turn relative to each other with the formation of a propeller-like structure in which there will be no place for additional molecules. In addition to increasing the steric load of the pyridyl substituents, it is necessary to make the paramagnetic tripod more symmetrical about the bridgehead carbon atom.

This can be done by going from a five-membered oxazolidine ring to a six-membered oxazinane (**41**), Figure 11a. The synthesis of such a tripodal radical becomes rather complicated due to commercially unavailable bis(6-methyl-2-pyridyl)methanone and 3-amino-3-methyl-butan-1-ol, the condensation of which yields its diamagnetic precursor.

Other way is a choice of 1-imidazole as a functional group (instead of pyridine) for oxazolidine nitroxide, Figure 11b. This is slightly easier root because the starting aminoalcohol is cheap, but corresponding bis-ketone must be prepared.

If the use of the hindered tripod **41** is intended to prevent coordination of hetero-ligands in the equatorial plane, which is favorable for complexes with oblate Ln-ions, then its unhindered congener is better to be used for heteroleptic complexes like **39** and **40** for the prolate series. The latter can also be chosen for heteroleptic complexes with tripod **42**.

 doi:10.20944/preprints202306.0983.v1

5. Conclusions

Despite numerous publications on the coordination chemistry of lanthanides with tripodal ligands containing detailed crystallographic information, their magnetic behavior has not been practically studied.

In contrast to the complexes of dysprosium and terbium, the coordination compounds of the prolate Pm, Sm, Er, Tm, and Yb are much less studied. For the latter, unhindered tripods with a shallow fit are more suitable, which makes it possible to ensure equatorial coordination of anionic hetero-ligands. Whereas sterically demanding tripods of the **4** type are brilliantly suited for obtaining stable divalent Ln complexes [44,92], which is especially promising for the design of magneto-luminescent materials based on Eu(II) complexes, because their tricationic congener Eu^{3+} has nonmagnetic ground state.

The review of complexes with diamagnetic tripodal ligands was made with the hope that physicochemists will pay attention to this family of compounds, and make more precisely magneto-structural predictions based on CF parameters for the lanthanide ions in the respective ligand environments.

In magnetic terms, mono- and biradical Ln-complexes are very interesting, but difficult for theoretical calculations. An important feature of potential materials is stability under normal conditions. Complexes with tripodal radicals possess this property. In addition, tripods have a predictable type of coordination, which is extremely important in the rational design of compounds with desired properties.

The strong magnetic interaction between the radical center and the metal ion has a number of advantages for the design of advanced SIMs. For example, an additional unpaired electron of an organic radical may transform the resulting cationic complex into the Kramers system, while free Ln has not this property. In addition, the direct interaction of the unpaired 2p electron of the radical with the 4f shell also removes the degeneracy of the energy levels, which can reduce QTM.

Without theoretical calculations, it is difficult to give precise prescriptions about the structure of the paramagnetic tripod for a particular lanthanide ion. However, we have tried to guess the general trend for cyclic nitroxyl radicals functionalized by aromatic nitrogen-containing heterocycles: pyridine and imidazoline.

Author Contributions: Not applicable

Funding: This research received no external funding" or "This research was funded by funded by Russian Science Foundation, Grant No. 23-23-00437 and partially supported by Ministry of Science and Higher Education of the Russian Federation (crystal structure determination for the complexes with nitroxide radicals, 121031700313-8)

Conflicts of Interest: The author declares no conflict of interest.

Data Availability Statement: Not applicable

References

1. Szczepura, L.F.; Witham, L.M.; Takeuchi, K.J. Tris(2-Pyridyl) Tripod Ligands. *Coord. Chem. Rev.* **1998**, *174*, 5–32, doi:10.1016/S0010-8545(98)00122-2.
2. Bellemin-Laponnaz, S.; Gade, L.H. A Modular Approach to C1 and C3 Chiral N-Tripodal Ligands for Asymmetric Catalysis. *Angew. Chemie Int. Ed.* **2002**, *41*, 3473–3475, doi:10.1002/1521-3773(20020916)41:18<3473::AID-ANIE3473>3.0.CO;2-N.
3. Natrajan, L.; Pécaut, J.; Mazzanti, M.; LeBrun, C. Controlled Hydrolysis of Lanthanide Complexes of the N-Donor Tripod Tris(2-Pyridylmethyl)Amine versus Bisligand Complex Formation. *Inorg. Chem.* **2005**, *44*, 4756–4765, doi:10.1021/ic0502224.
4. Chen, Y.-J.; Chen, H.-H. 1,1,1-Tris(Hydroxymethyl)Ethane as a New, Efficient, and Versatile Tripod Ligand for Copper-Catalyzed Cross-Coupling Reactions of Aryl Iodides with Amides, Thiols, and Phenols. *Org. Lett.* **2006**, *8*, 5609–5612, doi:10.1021/ol062339h.
5. Eckert, M.; Brethon, A.; Li, Y.-X.; Sheldon, R.A.; Arends, I.W.C.E. Study of the Efficiency of Amino-Functionalized Ruthenium and Ruthenacycle Complexes as Racemization Catalysts in the Dynamic Kinetic Resolution of 1-Phenylethanol. *Adv. Synth. Catal.* **2007**, *349*, 2603–2609, doi:10.1002/adsc.200700379.

6. Andrez, J.; Bozoklu, G.; Nocton, G.; Pécaut, J.; Scopelliti, R.; Dubois, L.; Mazzanti, M. Lanthanide(II) Complexes Supported by N,O-Donor Tripodal Ligands: Synthesis, Structure, and Ligand-Dependent Redox Behavior. *Chem. – A Eur. J.* **2015**, *21*, 15188–15200, doi:10.1002/chem.201502204.
7. Wietzke, R.; Mazzanti, M.; Latour, J.-M.; Pécaut, J.; Cordier, P.-Y.; Madic, C. Lanthanide(III) Complexes of Tripodal N-Donor Ligands: Structural Models for the Species Involved in Solvent Extraction of Actinides(III). *Inorg. Chem.* **1998**, *37*, 6690–6697, doi:10.1021/ic980192n.
8. Kuswandi, B.; N/a, N.; Verboom, W.; Reinhoudt, D.N. Tripodal Receptors for Cation and Anion Sensors. *Sensors* 2006, *6*, 978–1017.
9. Dai, Z.; Canary, J.W. Tailoring Tripodal Ligands for Zinc Sensing. *New J. Chem.* **2007**, *31*, 1708–1718, doi:10.1039/B710803F.
10. Machado, K.; Mukhopadhyay, S.; Videira, R.A.; Mishra, J.; Mobin, S.M.; Mishra, G.S. Polymer Encapsulated Scorpionate Eu^{3+} Complexes as Novel Hybrid Materials for High Performance Luminescence Applications. *RSC Adv.* **2015**, *5*, 35675–35682, doi:10.1039/C5RA02866C.
11. Yu, T.; Zhao, Y.; Fan, D.; Hong, Z.; Su, W. Preparation, Photo- and Electro-Luminescent Properties of a Novel Complex of Tb (III) with a Tripod Ligand. *Spectrochim. Acta Part A Mol. Biomol. Spectrosc.* **2008**, *69*, 654–658, doi: 10.1016/j.saa.2007.05.017.
12. Long, J.; Lyubov, D.M.; Mahrova, T. V.; Lyssenko, K.A.; Korlyukov, A.A.; Fedorov, Y. V.; Chernikova, E.Y.; Guari, Y.; Larionova, J.; Trifonov, A.A. Heteroleptic Lanthanide Complexes Coordinated by Tripodal Tetradentate Ligand: Synthesis, Structure, and Magnetic and Photoluminescent Properties. *Cryst. Growth Des.* **2020**, *20*, 5184–5192, doi: 10.1021/acs.cgd.0c00410.
13. Zhu, L.; Tang, H.; Harima, Y.; Yamashita, K.; Hirayama, D.; Aso, Y.; Otsubo, T. Electrochemical Properties of Self-Assembled Monolayers of Tripod-Shaped Molecules and Their Applications to Organic Light-Emitting Diodes. *Chem. Commun.* **2001**, 1830–1831, doi:10.1039/B105922J.
14. Zheng, X.-L.; Liu, Y.; Pan, M.; Lü, X.-Q.; Zhang, J.-Y.; Zhao, C.-Y.; Tong, Y.-X.; Su, C.-Y. Bright Blue-Emitting Ce3+ Complexes with Encapsulating Polybenzimidazole Tripodal Ligands as Potential Electroluminescent Devices. *Angew. Chemie Int. Ed.* **2007**, *46*, 7399–7403, doi:https://doi.org/10.1002/anie.200702401.
15. Chen, K.-Y.; Ivashenko, O.; Carroll, G.T.; Robertus, J.; Kistemaker, J.C.M.; London, G.; Browne, W.R.; Rudolf, P.; Feringa, B.L. Control of Surface Wettability Using Tripodal Light-Activated Molecular Motors. *J. Am. Chem. Soc.* **2014**, *136*, 3219–3224, doi:10.1021/ja412110t.
16. Kammerer, C.; Rapenne, G. Scorpionate Hydrotris(Indazolyl)Borate Ligands as Tripodal Platforms for Surface-Mounted Molecular Gears and Motors. *Eur. J. Inorg. Chem.* **2016**, *2016*, 2214–2226, doi:https://doi.org/10.1002/ejic.201501222.
17. Rabinovich, D. Synthetic Bioinorganic Chemistry: Scorpionates Turn 50 BT - 50 Years of Structure and Bonding – The Anniversary Volume. In; Mingos, D.M.P., Ed.; Springer International Publishing: Cham, 2017; pp. 139–157 ISBN 978-3-319-35138-4.
18. Eliseeva, S. V.; Bünzli, J.-C.G. Lanthanide Luminescence for Functional Materials and Bio-Sciences. *Chem. Soc. Rev.* **2010**, *39*, 189–227, doi:10.1039/B905604C.
19. Klitsche, F.; Ramcke, J.; Migenda, J.; Hensel, A.; Vossmeyer, T.; Weller, H.; Gross, S.; Maison, W. Synthesis of Tripodal Catecholates and Their Immobilization on Zinc Oxide Nanoparticles. *Beilstein J. Org. Chem.* **2015**, *11*, 678–686, doi:10.3762/bjoc.11.77.
20. A Fluorescent Sensor-Based Tripodal-Bodipy for Cu (II) Ions: Bio-Imaging on Cells. *TURKISH J. Chem.* **2021**, *45*, doi:10.3906/kim-2107-8.
21. Brechin, E.K. Using Tripodal Alcohols to Build High-Spin Molecules and Single-Molecule Magnets. *Chem. Commun.* **2005**, 5141–5153, doi:10.1039/B510102F.
22. Milios, C.J.; Manoli, M.; Rajaraman, G.; Mishra, A.; Budd, L.E.; White, F.; Parsons, S.; Wernsdorfer, W.; Christou, G.; Brechin, E.K. A Family of [Mn6] Complexes Featuring Tripodal Ligands. *Inorg. Chem.* **2006**, *45*, 6782–6793, doi:10.1021/ic060676g.
23. Domingo, N.; Bellido, E.; Ruiz-Molina, D. Advances on Structuring, Integration and Magnetic Characterization of Molecular Nanomagnets on Surfaces and Devices. *Chem. Soc. Rev.* **2012**, *41*, 258–302, doi:10.1039/C1CS15096K.
24. Long, J.; Lyubov, D.M.; Mahrova, T. V.; Cherkasov, A. V.; Fukin, G.K.; Guari, Y.; Larionova, J.; Trifonov, A.A. Synthesis, Structure and Magnetic Properties of Tris(Pyrazolyl)Methane Lanthanide Complexes: Effect of the Anion on the Slow Relaxation of Magnetization. *Dalt. Trans.* **2018**, *47*, 5153–5156, doi:10.1039/C8DT00458G.
25. Ito, A.; Nakano, Y.; Urabe, M.; Tanaka, K.; Shiro, M. Structural and Magnetic Studies of Copper(II) and Zinc(II) Coordination Complexes Containing Nitroxide Radicals as Chelating Ligands. *Eur. J. Inorg. Chem.* **2006**, *2006*, 3359–3368, doi: 10.1002/ejic.200600085.
26. Gass, I.A.; Gartshore, C.J.; Lupton, D.W.; Moubaraki, B.; Nafady, A.; Bond, A.M.; Boas, J.F.; Cashion, J.D.; Milsmann, C.; Wieghardt, K.; et al. Anion Dependent Redox Changes in Iron Bis-Terdentate Nitroxide {NNO} Chelates. *Inorg. Chem.* **2011**, *50*, 3052–3064, doi:10.1021/ic102588h.
27. Gass, I.A.; Tewary, S.; Nafady, A.; Chilton, N.F.; Gartshore, C.J.; Asadi, M.; Lupton, D.W.; Moubaraki, B.; Bond, A.M.; Boas, J.F.; et al. Observation of Ferromagnetic Exchange, Spin Crossover, Reductively Induced

Oxidation, and Field-Induced Slow Magnetic Relaxation in Monomeric Cobalt Nitroxides. *Inorg. Chem.* **2013**, *52*, 7557–7572, doi:10.1021/ic400565h.

28. Gass, I.A.; Tewary, S.; Rajaraman, G.; Asadi, M.; Lupton, D.W.; Moubaraki, B.; Chastanet, G.; Létard, J.-F.; Murray, K.S. Solvate-Dependent Spin Crossover and Exchange in Cobalt(II) Oxazolidine Nitroxide Chelates. *Inorg. Chem.* **2014**, *53*, 5055–5066, doi:10.1021/ic5001057.
29. Gass, I.A.; Asadi, M.; Lupton, D.W.; Moubaraki, B.; Bond, A.M.; Guo, S.-X.; Murray, K.S. Manganese(II) Oxazolidine Nitroxide Chelates: Structure, Magnetism, and Redox Properties. *Aust. J. Chem.* **2014**, *67*, 1618, doi:10.1071/CH14390.
30. Pedersen, A.H.; Geoghegan, B.L.; Nichol, G.S.; Lupton, D.W.; Murray, K.S.; Martínez-Lillo, J.; Gass, I.A.; Brechin, E.K. Hexahalorhenate(IV) Salts of Metal Oxazolidine Nitroxides. *Dalt. Trans.* **2017**, *46*, 5250–5259, doi: 10.1039/C7DT00752C.
31. Gass, I.A.; Lu, J.; Asadi, M.; Lupton, D.W.; Forsyth, C.M.; Geoghegan, B.L.; Moubaraki, B.; Cashion, J.D.; Martin, L.L.; Bond, A.M.; et al. Use of the TCNQF 4 2− Dianion in the Spontaneous Redox Formation of [Fe III (L −) 2][TCNQF 4 ·−]. *Chempluschem* **2018**, *83*, 658–668, doi:10.1002/cplu.201800010.
32. Gass, I.A.; Lu, J.; Ojha, R.; Asadi, M.; Lupton, D.W.; Geoghegan, B.L.; Moubaraki, B.; Martin, L.L.; Bond, A.M.; Murray, K.S. [FeII(L•)2][TCNQF4•−]2: A Redox-Active Double Radical Salt. *Aust. J. Chem.* **2019**, *72*, 769–777, doi:10.1071/CH19175.
33. Trofimenko, S. Boron-Pyrazole Chemistry. *J. Am. Chem. Soc.* **1966**, *88*, 1842–1844, doi:10.1021/ja00960a065.
34. Oliver, J.D.; Mullica, D.F.; Hutchinson, B.B.; Milligan, W.O. Iron-Nitrogen Bond Lengths in Low-Spin and High-Spin Iron(II) Complexes with Poly(Pyrazolyl)Borate Ligands. *Inorg. Chem.* **1980**, *19*, 165–169, doi:10.1021/ic50203a034.
35. Trofimenko, S. Recent Advances in Poly(Pyrazolyl)Borate (Scorpionate) Chemistry. *Chem. Rev.* **1993**, *93*, 943–980, doi:10.1021/cr00019a006.
36. Wu, L.P.; Yamagiwa, Y.; Ino, I.; Sugimoto, K.; Kuroda-Sowa, T.; Kamikawa, T.; Munakata, M. Unique Tetranuclear Copper(II) Cluster and Monomeric Iron(II), (III) Complexes with a Tris(Imidazolyl) Chelating Ligand. *Polyhedron* **1999**, *18*, 2047–2053, doi:10.1016/S0277-5387(99)00083-2.
37. *SCORPIONATES II: CHELATING BORATE LIGANDS - Dedicated To Swiatoslaw Trofimenko*; Pettinari, C., Ed.; IMPERIAL COLLEGE PRESS and distribiuted by World Scientific: London, 2008; ISBN 978-1-86094-876-3.
38. Dougherty, W.G.; Kassel, W.S. Synthesis of a Series of First-Row Tris-Imidazolylphosphine Sandwich Complexes and Their Potential for Formation of Polymetallic Species. *Inorganica Chim. Acta* **2010**, *364*, 120–124, doi: 10.1016/j.ica.2010.08.012.
39. Saouma, C.T.; Peters, J.C. ME and ME Complexes of Iron and Cobalt That Emphasize Three-Fold Symmetry (E=O, N, NR). *Coord. Chem. Rev.* **2011**, *255*, 920–937, doi:https://doi.org/10.1016/j.ccr.2011.01.009.
40. Lavrenova, L.G.; Strekalova, A.D.; Smolentsev, A.I.; Naumov, D.Y.; Bogomyakov, A.S.; Sheludyakova, L.A.; Vasilevskii, S.F. Mono- and Heteroligand Iron(II) Complexes with Tris(3,5-Dimethylpyrazol-1-Yl)Methane. *Russ. J. Coord. Chem.* **2016**, *42*, 711–718, doi:10.1134/S107032841611004X.
41. Feng, M.; Tong, M.-L. Single Ion Magnets from 3d to 5f: Developments and Strategies. *Chem. – A Eur. J.* **2018**, *24*, 7574–7594, doi:https://doi.org/10.1002/chem.201705761.
42. Landart-Gereka, A.; Quesada-Moreno, M.M.; Palacios, M.A.; Díaz-Ortega, I.F.; Nojiri, H.; Ozerov, M.; Krzystek, J.; Colacio, E. Pushing up the Easy-Axis Magnetic Anisotropy and Relaxation Times in Trigonal Prismatic Co^{II} Mononuclear SMMs by Molecular Structure Design. *Chem. Commun.* **2023**, *59*, 952–955, doi:10.1039/D2CC06012D.
43. Apostolidis, C.; Carvalho, A.; Domingos, A.; Kanellakopulos, B.; Maier, R.; Marques, N.; Matos, A.P. de; Rebizant, J. Chloro-Lanthanide, and Plutonium Complexes Containing the Hydrotris (3,5-Dimethylpyrazol-1-Yl)Borate Ligand: The Crystal and Molecular Structures of [PrCl(μ-Cl)$TpMe_2$(3,5-Me_2pzH)]$_2$ and $YbCl_2TpMe_2$ (THF). *Polyhedron* **1998**, *18*, 263–272, doi: 10.1016/S0277-5387(98)00294-0.
44. Hillier, A.C.; Zhang, X.W.; Maunder, G.H.; Liu, S.Y.; Eberspacher, T.A.; Metz, M. V.; McDonald, R.; Domingos, A.; Marques, N.; Day, V.W.; et al. Synthesis and Structural Comparison of a Series of Divalent Ln(TpR,R)$_2$ (Ln = Sm, Eu, Yb) and Trivalent Sm($TpMe_2$)$_2$X (X = F, Cl, I, BPh_4) Complexes. *Inorg. Chem.* **2001**, *40*, 5106–5116, doi:10.1021/ic010325w.
45. Sella, A.; Brown, S.E.; Steed, J.W.; Tocher, D.A. Synthesis and Solid-State Structures of Pyrazolylmethane Complexes of the Rare Earths. *Inorg. Chem.* **2007**, *46*, 1856–1864, doi:10.1021/ic062370f.
46. Liu, S.-Y.; Maunder, G.H.; Sella, A.; Stevenson, M.; Tocher, D.A. Synthesis and Molecular Structures of Hydrotris(Dimethylpyrazolyl)Borate Complexes of the Lanthanides. *Inorg. Chem.* **1996**, *35*, 76–81, doi:10.1021/ic941469w.
47. Werner, E.J.; Biros, S.M. Supramolecular Ligands for the Extraction of Lanthanide and Actinide Ions. *Org. Chem. Front.* **2019**, *6*, 2067–2094, doi:10.1039/C9QO00242A.
48. Barraza, R.; Sertage, A.G.; Kajjam, A.B.; Ward, C.L.; Lutter, J.C.; Schlegel, H.B.; Allen, M.J. Properties of Amine-Containing Ligands That Are Necessary for Visible-Light-Promoted Catalysis with Divalent Europium. *Inorg. Chem.* **2022**, *61*, 19649–19657, doi:10.1021/acs.inorgchem.2c02911.

49. Frost, J.M.; Harriman, K.L.M.; Murugesu, M. The Rise of 3-d Single-Ion Magnets in Molecular Magnetism: Towards Materials from Molecules? *Chem. Sci.* **2016**, *7*, 2470–2491, doi:10.1039/C5SC03224E.
50. Zhu, Z.; Guo, M.; Li, X.-L.; Tang, J. Molecular Magnetism of Lanthanide: Advances and Perspectives. *Coord. Chem. Rev.* **2019**, *378*, 350–364, doi:10.1016/j.ccr.2017.10.030.
51. Zabala-Lekuona, A.; Seco, J.M.; Colacio, E. Single-Molecule Magnets: From Mn12-Ac to Dysprosium Metallocenes, a Travel in Time. *Coord. Chem. Rev.* **2021**, *441*, 213984, doi:10.1016/j.ccr.2021.213984.
52. Gatteschi, D.; Sessoli, R. Quantum Tunneling of Magnetization and Related Phenomena in Molecular Materials. *Angew. Chemie Int. Ed.* **2003**, *42*, 268–297, doi:10.1002/anie.200390099.
53. Goodwin, C.A.P.; Ortu, F.; Reta, D. Strangely Attractive: Collaboration and Feedback in the Field of Molecular Magnetism. *Int. J. Quantum Chem.* **2020**, *120*, e26248, doi:https://doi.org/10.1002/qua.26248.
54. Tang, J.; Zhang, P. *Lanthanide Single Molecule Magnets*; Springer Berlin Heidelberg: Berlin, Heidelberg, 2015; ISBN 978-3-662-46998-9.
55. Sorace, L.; Gatteschi, D. Electronic Structure and Magnetic Properties of Lanthanide Molecular Complexes. In *Lanthanides and Actinides in Molecular Magnetism*; Wiley-VCH Verlag GmbH & Co. KGaA: Weinheim, Germany, 2015; pp. 1–26.
56. Goodwin, C.A.P.; Ortu, F.; Reta, D.; Chilton, N.F.; Mills, D.P. Molecular Magnetic Hysteresis at 60 Kelvin in Dysprosocenium. *Nature* **2017**, *548*, 439–442, doi:10.1038/nature23447.
57. Guo, F.-S.; Day, B.M.; Chen, Y.-C.; Tong, M.-L.; Mansikkamäki, A.; Layfield, R.A. A Dysprosium Metallocene Single-Molecule Magnet Functioning at the Axial Limit. *Angew. Chemie Int. Ed.* **2017**, *56*, 11445–11449, doi:10.1002/anie.201705426.
58. Guo, F.-S.; Day, B.M.; Chen, Y.-C.; Tong, M.-L.; Mansikkamäki, A.; Layfield, R.A. Magnetic Hysteresis up to 80 Kelvin in a Dysprosium Metallocene Single-Molecule Magnet. *Science (80-.).* **2018**, *362*, 1400–1403, doi:10.1126/science.aav0652.
59. Vincent, A.H.; Whyatt, Y.L.; Chilton, N.F.; Long, J.R. Strong Axiality in a Dysprosium(III) Bis(Borolide) Complex Leads to Magnetic Blocking at 65 K. *J. Am. Chem. Soc.* **2023**, *145*, 1572–1579, doi:10.1021/jacs.2c08568.
60. Rinehart, J.D.; Long, J.R. Exploiting Single-Ion Anisotropy in the Design of f-Element Single-Molecule Magnets. *Chem. Sci.* **2011**, *2*, 2078–2085, doi:10.1039/C1SC00513H.
61. Chilton, N.F. Design Criteria for High-Temperature Single-Molecule Magnets. *Inorg. Chem.* **2015**, *54*, 2097–2099, doi:10.1021/acs.inorgchem.5b00089.
62. Harriman, K.L.M.; Errulat, D.; Murugesu, M. Magnetic Axiality: Design Principles from Molecules to Materials. *Trends Chem.* **2019**, *1*, 425–439, doi:10.1016/j.trechm.2019.04.005.
63. Guo, F.-S.; Bar, A.K.; Layfield, R.A. Main Group Chemistry at the Interface with Molecular Magnetism. *Chem. Rev.* **2019**, *119*, 8479–8505, doi:10.1021/acs.chemrev.9b00103.
64. Chiesa, A.; Cugini, F.; Hussain, R.; Macaluso, E.; Allodi, G.; Garlatti, E.; Giansiracusa, M.; Goodwin, C.A.P.; Ortu, F.; Reta, D.; et al. Understanding Magnetic Relaxation in Single-Ion Magnets with High Blocking Temperature. *Phys. Rev. B* **2020**, *101*, 174402, doi:10.1103/PhysRevB.101.174402.
65. Woodruff, D.N.; Winpenny, R.E.P.; Layfield, R.A. Lanthanide Single-Molecule Magnets. *Chem. Rev.* **2013**, *113*, 5110–5148, doi:10.1021/cr400018q.
66. Jiang, S.-D.; Wang, B.-W.; Gao, S. Advances in Lanthanide Single-Ion Magnets BT - Molecular Nanomagnets and Related Phenomena. In; Gao, S., Ed.; Springer Berlin Heidelberg: Berlin, Heidelberg, 2015; pp. 111–141 ISBN 978-3-662-45723-8.
67. Gupta, S.K.; Murugavel, R. Enriching Lanthanide Single-Ion Magnetism through Symmetry and Axiality. *Chem. Commun.* **2018**, *54*, 3685–3696, doi:10.1039/C7CC09956H.
68. Vogel, R.; Müntener, T.; Häussinger, D. Intrinsic Anisotropy Parameters of a Series of Lanthanoid Complexes Deliver New Insights into the Structure-Magnetism Relationship. *Chem* **2021**, *7*, 3144–3156, doi: 10.1016/j.chempr.2021.08.011.
69. Jiang, S.-D.; Qin, S.-X. Prediction of the Quantized Axis of Rare-Earth Ions: The Electrostatic Model with Displaced Point Charges. *Inorg. Chem. Front.* **2015**, *2*, 613–619, doi:10.1039/C5QI00052A.
70. Liu, J.-L.; Chen, Y.-C.; Tong, M.-L. Symmetry Strategies for High Performance Lanthanide-Based Single-Molecule Magnets. *Chem. Soc. Rev.* **2018**, *47*, 2431–2453, doi:10.1039/C7CS00266A.
71. Chen, Y.-C.; Tong, M.-L. Single-Molecule Magnets beyond a Single Lanthanide Ion: The Art of Coupling. *Chem. Sci.* **2022**, doi:10.1039/D2SC01532C.
72. *Molecular Nanomagnets and Related Phenomena —Structure and Bonding*; Gao, S., Ed.; Springer Berlin: Heidelberg, 2015; ISBN 978-3-662-45722-1.
73. Kahn, O. *Molecular Magnetism*; VCH: New York, NY, USA, 1993; ISBN 978-1-56081-566-2.
74. Series Page. In *Theoretical Foundations of Molecular Magnetism*; Boča, R.B.T.-C.M. in I.C., Ed.; Elsevier, 1999; Vol. 1, p. ii ISBN 1873-0418.
75. Chen, Y.-C.; Liu, J.-L.; Wernsdorfer, W.; Liu, D.; Chibotaru, L.F.; Chen, X.-M.; Tong, M.-L. Hyperfine-Interaction-Driven Suppression of Quantum Tunneling at Zero Field in a Holmium(III) Single-Ion Magnet. *Angew. Chemie Int. Ed.* **2017**, *56*, 4996–5000, doi:https://doi.org/10.1002/anie.201701480.

76. Skomski, R.; Sellmyer, D.J. Anisotropy of Rare-Earth Magnets. *J. Rare Earths* **2009**, *27*, 675–679, doi:10.1016/S1002-0721(08)60314-2.
77. Zhu, Z.; Tang, J. Lanthanide Single-Molecule Magnets with High Anisotropy Barrier: Where to from Here? *Natl. Sci. Rev.* **2022**, *9*, nwac194, doi:10.1093/nsr/nwac194.
78. Wang, J.; Sun, C.; Zheng, Q.; Wang, D.; Chen, Y.; Ju, J.; Sun, T.; Cui, Y.; Ding, Y.; Tang, Y. Lanthanide Single-molecule Magnets: Synthetic Strategy, Structures, Properties and Recent Advances. *Chem. – An Asian J.* **2023**, *18*, doi:10.1002/asia.202201297.
79. Trofimenko, S. *The Coordination Chemistry of Polypyrazolylborate Ligand*; IMPERIAL COLLEGE PRESS, 1999; ISBN 978-1-86094-172-6.
80. Cheng, J.; Takats, J.; Ferguson, M.J.; McDonald, R. Heteroleptic Tm(II) Complexes: One More Success for Trofimenko's Scorpionates. *J. Am. Chem. Soc.* **2008**, *130*, 1544–1545, doi:10.1021/ja0776273.
81. Dei, A.; Gatteschi, D.; Pécaut, J.; Poussereau, S.; Sorace, L.; Vostrikova, K. Crystal Field and Exchange Effects in Rare Earth Semiquinone Complexes. *Comptes Rendus l'Academie des Sci. - Ser. IIC Chem.* **2001**, *4*, doi:10.1016/S1387-1609(00)01196-8.
82. Zhang, P.; Perfetti, M.; Kern, M.; Hallmen, P.P.; Ungur, L.; Lenz, S.; Ringenberg, M.R.; Frey, W.; Stoll, H.; Rauhut, G.; et al. Exchange Coupling and Single Molecule Magnetism in Redox-Active Tetraoxolene-Bridged Dilanthanide Complexes. *Chem. Sci.* **2018**, *9*, 1221–1230, doi:10.1039/C7SC04873D.
83. Xu, G.-F.; Gamez, P.; Tang, J.; Clérac, R.; Guo, Y.-N.; Guo, Y. MIIIDyIII3 (M = FeIII, CoIII) Complexes: Three-Blade Propellers Exhibiting Slow Relaxation of Magnetization. *Inorg. Chem.* **2012**, *51*, 5693–5698, doi:10.1021/ic300126q.
84. Xu, G.-F.; Wang, Q.-L.; Gamez, P.; Ma, Y.; Clérac, R.; Tang, J.; Yan, S.-P.; Cheng, P.; Liao, D.-Z. A Promising New Route towards Single-Molecule Magnets Based on the Oxalate Ligand. *Chem. Commun.* **2010**, *46*, 1506–1508, doi:10.1039/B920215C.
85. Mikhalyova, E.A.; Zeller, M.; Jasinski, J.P.; Butcher, R.J.; Carrella, L.M.; Sedykh, A.E.; Gavrilenko, K.S.; Smola, S.S.; Frasso, M.; Cazorla, S.C.; et al. Combination of Single-Molecule Magnet Behaviour and Luminescence Properties in a New Series of Lanthanide Complexes with Tris(Pyrazolyl)Borate and Oligo(β-Diketonate) Ligands. *Dalt. Trans.* **2020**, *49*, 7774–7789, doi:10.1039/D0DT00600A.
86. Kandel, A. V.; Mikhalyova, E.A.; Zeller, M.; Addison, A.W.; Pavlishchuk, V. V. Influence of the Structure of 3-Arylacetylacetonate Ligands on the Luminescence Properties of Eu3+ and Tb3+ Complexes. *Theor. Exp. Chem.* **2017**, *53*, 180–186, doi:10.1007/s11237-017-9513-y.
87. Depperman, E.C.; Bodnar, S.H.; Vostrikova, K.E.; Shultz, D.A.; Kirk, M.L. Spin Robustness of a New Hybrid Inorganic−Organic High-Spin Molecule. *J. Am. Chem. Soc.* **2001**, *123*, 3133–3134, doi:10.1021/ja003739h.
88. Wang, S.; Zuo, J.-L.; Zhou, H.-C.; Choi, H.J.; Ke, Y.; Long, J.R.; You, X.-Z. $[(Tp)_8(H_2O)_6Cu^{II}_6Fe^{III}_8(CN)_{24}]^{4+}$: A Cyanide-Bridged Face-Centered-Cubic Cluster with Single-Molecule-Magnet Behavior. *Angew. Chemie Int. Ed.* **2004**, *43*, 5940–5943, doi:10.1002/anie.200461515.
89. Wang, S.; Zuo, J.-L.; Gao, S.; Song, Y.; Zhou, H.-C.; Zhang, Y.-Z.; You, X.-Z. The Observation of Superparamagnetic Behavior in Molecular Nanowires. *J. Am. Chem. Soc.* **2004**, *126*, 8900–8901, doi:10.1021/ja0483995.
90. Alexandropoulos, D.I.; Vignesh, K.R.; Xie, H.; Dunbar, K.R. Switching on Single-Molecule Magnet Properties of Homoleptic Sandwich Tris(Pyrazolyl)Borate Dysprosium(III) Cations *via* Intermolecular Dipolar Coupling. *Dalt. Trans.* **2019**, *48*, 10610–10618, doi:10.1039/C9DT00597H.
91. Kühling, M.; Wickleder, C.; Ferguson, M.J.; Hrib, C.G.; McDonald, R.; Suta, M.; Hilfert, L.; Takats, J.; Edelmann, F.T. Investigation of the "Bent Sandwich-like" Divalent Lanthanide Hydro-Tris(Pyrazolyl)Borates $Ln(TpIPr_2)_2$ (Ln = Sm, Eu, Tm, Yb). *New J. Chem.* **2015**, *39*, 7617–7625, doi:10.1039/C5NJ00568J.
92. Qi, H.; Zhao, Z.; Zhan, G.; Sun, B.; Yan, W.; Wang, C.; Wang, L.; Liu, Z.; Bian, Z.; Huang, C. Air Stable and Efficient Rare Earth Eu(II) Hydro-Tris(Pyrazolyl)Borate Complexes with Tunable Emission Colors. *Inorg. Chem. Front.* **2020**, *7*, 4593–4599, doi:10.1039/D0QI00762E.
93. Takats, J.; Zhang, X.W.; Day, V.W.; Eberspacher, T.A. Synthesis and Structure of Bis[Hydrotris(3,5-Dimethylpyrazolyl)Borato]Samarium(II), $Sm[HB(3,5\text{-}Me_2pz)_3]_2$, and the Product of Its Reaction with Azobenzene. *Organometallics* **1993**, *12*, 4286–4288, doi:10.1021/om00035a011.
94. Maunder, G.H.; Sella, A.; Tocher, D.A. Synthesis and Molecular Structures of a Redox-Related Pair of Lanthanide Complexes. *J. Chem. Soc. Chem. Commun.* **1994**, 885, doi:10.1039/c39940000885.
95. Momin, A.; Carter, L.; Yang, Y.; McDonald, R.; Essafi (née Labouille), S.; Nief, F.; Del Rosal, I.; Sella, A.; Maron, L.; Takats, J. To Bend or Not To Bend: Experimental and Computational Studies of Structural Preference in $Ln(TpiPr_2)_2$ (Ln = Sm, Tm). *Inorg. Chem.* **2014**, *53*, 12066–12075, doi:10.1021/ic501816v.
96. Saliu, K.O.; Takats, J.; Ferguson, M.J. Bis[Tris(3-Tert-Butyl-5-Methylpyrazol-1-Yl)Hydridoborato]Ytterbium(II) Toluene Solvate. *Acta Crystallogr. Sect. E Struct. Reports Online* **2009**, *65*, m643–m644, doi:10.1107/S1600536809017152.
97. Suta, M.; Kühling, M.; Liebing, P.; Edelmann, F.T.; Wickleder, C. Photoluminescence Properties of the "Bent Sandwich-like" Compounds $[Eu(TpIPr_2)_2]$ and $[Yb(TpIPr_2)_2]^-$ Intermediates between Nitride-Based Phosphors and Metallocenes. *J. Lumin.* **2017**, *187*, 62–68, doi:10.1016/j.jlumin.2017.02.054.

98. Arikawa, Y.; Inada, K.; Onishi, M. Side-on Coordination Mode of a Pyrazolyl Group in the Structure of a Divalent [Sm{B(3-Mepz)$_4$}$_2$] Complex (3-Mepz Is 3-Methylpyrazol-1-Yl). *Acta Crystallogr. Sect. C Struct. Chem.* **2016**, *72*, 838–841, doi:10.1107/S2053229616011578.
99. Li, Z.-H.; Zhai, Y.-Q.; Chen, W.-P.; Ding, Y.-S.; Zheng, Y.-Z. Air-Stable Hexagonal Bipyramidal Dysprosium(III) Single-Ion Magnets with Nearly Perfect D_{6h} Local Symmetry. *Chem. – A Eur. J.* **2019**, *25*, 16219–16224, doi: 10.1002/chem.201904325.
100. Canaj, A.B.; Dey, S.; Martí, E.R.; Wilson, C.; Rajaraman, G.; Murrie, M. Insight into D 6 h Symmetry: Targeting Strong Axiality in Stable Dysprosium(III) Hexagonal Bipyramidal Single-Ion Magnets. *Angew. Chemie Int. Ed.* **2019**, *58*, 14146–14151, doi:10.1002/anie.201907686.
101. Li, Q.-W.; Wan, R.-C.; Chen, Y.-C.; Liu, J.-L.; Wang, L.-F.; Jia, J.-H.; Chilton, N.F.; Tong, M.-L. Unprecedented Hexagonal Bipyramidal Single-Ion Magnets Based on Metallacrowns. *Chem. Commun.* **2016**, *52*, 13365–13368, doi:10.1039/C6CC06924J.
102. Gil, Y.; Castro-Alvarez, A.; Fuentealba, P.; Spodine, E.; Aravena, D. Lanthanide SMMs Based on Belt Macrocycles: Recent Advances and General Trends. *Chem. – A Eur. J.* **2022**, *28*, e202200336, doi:https://doi.org/10.1002/chem.202200336.
103. Meyer, G. All the Lanthanides Do It and Even Uranium Does Oxidation State +2. *Angew. Chemie Int. Ed.* **2014**, *53*, 3550–3551, doi:https://doi.org/10.1002/anie.201311325.
104. Llunell, M.; Casanova, D.; Cirera, J.; Alemany, P.; Alvarez, S. SHAPE, Version 2.1, Program for the Stereochemical Analysis of Molecular Fragments by Means of Continuous Shape Measures and Associated Tools. *Univ. Barcelona, Barcelona, Spain* **2013**, *2103*.
105. Li, T.; Zhang, G.; Guo, J.; Wang, S.; Leng, X.; Chen, Y. Tris(Pyrazolyl)Methanide Complexes of Trivalent Rare-Earth Metals. *Organometallics* **2016**, *35*, 1565–1572, doi:10.1021/acs.organomet.6b00166.
106. Keene, F.R.; Snow, M.R.; Stephenson, P.J.; Tiekink, E.R.T. Ruthenium(II) Complexes of the C_{3v} Ligands Tris(2-Pyridyl)Amine, Tris(2-Pyridyl)Methane, and Tris(2-Pyridyl)Phosphine. 1. Synthesis and x-Ray Structural Studies of the Bis(Ligand) Complexes. *Inorg. Chem.* **1988**, *27*, 2040–2045, doi:10.1021/ic00285a010.
107. García, F.; Hopkins, A.D.; Humphrey, S.M.; McPartlin, M.; Rogers, M.C.; Wright, D.S. The First Example of a Si-Bridged Tris(Pyridyl) Ligand; Synthesis and Structure of [MeSi(2-C_5H_4N)$_3$LiX] (X = 0.2Br, 0.8Cl). *Dalt. Trans.* **2004**, 361–362, doi: 10.1039/B315503J.
108. MANN, F.G.; WATSON, J. Conditions of Salt Formation in Polyamines And Kindred Compounds. Salt Formation in the Tertiary 2-Pyridylamines, Phosphines and Arsines. *J. Org. Chem.* **1948**, *13*, 502–531, doi:10.1021/jo01162a007.
109. García, F.; Hopkins, A.D.; Kowenicki, R.A.; McPartlin, M.; Rogers, M.C.; Silvia, J.S.; Wright, D.S. Syntheses and Structure of Heterometallic Complexes Containing Tripodal Group 13 Ligands [RE(2-Py)3]- (E = Al, In). *Organometallics* **2006**, *25*, 2561–2568, doi:10.1021/om0600691.
110. Beswick, M.A.; Belle, C.J.; Davies, M.K.; Halcrow, M.A.; Raithby, P.R.; Steiner, A.; Wright, D.S. One-Pot Synthesis of a Novel Tridentate Tin(IV) Ligand; Syntheses and Structures of [BunSn(NC5H4-C,N)3MBr](M = Li, Cu). *Chem. Commun.* **1996**, 2619, doi:10.1039/cc9960002619.
111. Zeckert, K.; Zahn, S.; Kirchner, B. Tin–Lanthanoid Donor–Acceptor Bonds. *Chem. Commun.* **2010**, *46*, 2638, doi: 10.1039/b924967b.
112. Beswick, M.A.; Davies, M.K.; Raithby, P.R.; Steiner, A.; Wright, D.S. Synthesis and Structure of [Pb(2-Py)$_3$Li·THF], Containing a Low-Valent Group 14 Tris(Pyridyl) Ligand (2-Py = 2-Pyridyl). *Organometallics* **1997**, *16*, 1109–1110, doi:10.1021/om9609123.
113. Goura, J.; McQuade, J.; Shimoyama, D.; Lalancette, R.A.; Sheridan, J.B.; Jäkle, F. Electrophilic and Nucleophilic Displacement Reactions at the Bridgehead Borons of Tris(Pyridyl)Borate Scorpionate Complexes. *Chem. Commun.* **2022**, *58*, 977–980, doi:10.1039/D1CC06181J.
114. Reichart, F.; Kischel, M.; Zeckert, K. Lanthanide(II) Complexes of a Dual Functional Tris(2-Pyridyl)Stannate Derivative. *Chem. – A Eur. J.* **2009**, *15*, 10018–10020, doi:10.1002/chem.200901286.
115. Zeckert, K. Syntheses and Structures of Lanthanoid(Ii) Complexes Featuring Sn–M (M = Al, Ga, In) Bonds. *Dalt. Trans.* **2012**, *41*, 14101–14106, doi:10.1039/C2DT31768K.
116. Zeckert, K. Pyridyl Compounds of Heavier Group 13 and 14 Elements as Ligands for Lanthanide Metals. *Organometallics* **2013**, *32*, 1387–1393, doi:10.1021/om301032x.
117. Zeckert, K.; Griebel, J.; Kirmse, R.; Weiß, M.; Denecke, R. Versatile Reactivity of a Lithium Tris(Aryl)Plumbate(II) Towards Organolanthanoid Compounds: Stable Lead-Lanthanoid-Metal Bonds or Redox Processes. *Chem. - A Eur. J.* **2013**, *19*, 7718–7722, doi:10.1002/chem.201300596.
118. Hellmann, K.W.; Gade, L.H.; Gevert, O.; Steinert, P.; Lauher, J.W. Tripodal Triamidostannates and -Plumbates. *Inorg. Chem.* **1995**, *34*, 4069–4078, doi:10.1021/ic00120a010.
119. García-Rodríguez, R.; Simmonds, H.R.; Wright, D.S. Formation of a Heterometallic AlIII/SmIII Complex Involving a Novel [EtAl(2-Py)$_2$O]$^{2-}$ Ligand (2-Py = 2-Pyridyl). *Organometallics* **2014**, *33*, 7113–7117, doi:10.1021/om5009132.
120. García-Rodríguez, R.; Kopf, S.; Wright, D.S. Modifying the Donor Properties of Tris(Pyridyl)Aluminates in Lanthanide(Ii) Sandwich Compounds. *Dalt. Trans.* **2018**, *47*, 2232–2239, doi:10.1039/C7DT04657J.

121. Hajiashrafi, T.; Nemati Kharat, A.; Love, J.A.; Patrick, B.O. Synthesis, Characterization and Crystal Structure of Three New Lanthanide (III) Complexes with the [(6-Methyl-2-Pyridyl)Methyl]Bis(2-Pyridylmethyl)Amine (MeTPA) Ligand; New Precursors for Lanthanide (III) Oxide Nano-Particles. *Polyhedron* **2013**, *60*, 30–38, doi:10.1016/j.poly.2013.04.061.
122. Hay, M.A.; Gable, R.W.; Boskovic, C. Modulating the Electronic Properties of Divalent Lanthanoid Complexes with Subtle Ligand Tuning. *Dalt. Trans.* **2023**, *52*, 3315–3324, doi:10.1039/D2DT03782C.
123. Zhang, C.; Cheng, Z.; Tan, P.; Lv, W.; Cui, H.; Chen, L.; Cai, X.; Zhao, Y.; Yuan, A. Tuning the Ligand Field in Seven-Coordinate Dy(III) Complexes to Perturb Single-Ion Magnet Behavior. *New J. Chem.* **2021**, *45*, 8591–8596, doi: 10.1039/D1NJ00734C.
124. Demir, S.; Jeon, I.-R.; Long, J.R.; Harris, T.D. Radical Ligand-Containing Single-Molecule Magnets. *Coord. Chem. Rev.* **2015**, *289–290*, 149–176, doi:10.1016/j.ccr.2014.10.012.
125. Ishikawa, N.; Sugita, M.; Tanaka, N.; Ishikawa, T.; Koshihara, S.; Kaizu, Y. Upward Temperature Shift of the Intrinsic Phase Lag of the Magnetization of Bis(Phthalocyaninato)Terbium by Ligand Oxidation Creating an S = 1 / 2 Spin. *Inorg. Chem.* **2004**, *43*, 5498–5500, doi:10.1021/ic049348b.
126. Pederson, R.; Wysocki, A.L.; Mayhall, N.; Park, K. Multireference Ab Initio Studies of Magnetic Properties of Terbium-Based Single-Molecule Magnets. *J. Phys. Chem. A* **2019**, *123*, 6996–7006, doi:10.1021/acs.jpca.9b03708.
127. Rinehart, J.D.; Fang, M.; Evans, W.J.; Long, J.R. A N 2 3– Radical-Bridged Terbium Complex Exhibiting Magnetic Hysteresis at 14 K. *J. Am. Chem. Soc.* **2011**, *133*, 14236–14239, doi:10.1021/ja206286h.
128. Rinehart, J.D.; Fang, M.; Evans, W.J.; Long, J.R. Strong Exchange and Magnetic Blocking in N23−-Radical-Bridged Lanthanide Complexes. *Nat. Chem.* **2011**, *3*, 538–542, doi:10.1038/nchem.1063.
129. Vieru, V.; Iwahara, N.; Ungur, L.; Chibotaru, L.F. Giant Exchange Interaction in Mixed Lanthanides. *Sci. Rep.* **2016**, *6*, 24046, doi:10.1038/srep24046.
130. Eugene V Tretyakov; Victor I Ovcharenko The Chemistry of Nitroxide Radicals in the Molecular Design of Magnets. *Russ. Chem. Rev.* **2009**, *78*, 971, doi:10.1070/RC2009v078n11ABEH004093.
131. Vostrikova, K.E. High-Spin Molecules Based on Metal Complexes of Organic Free Radicals. *Coord. Chem. Rev.* **2008**, *252*, 1409–1419, doi:10.1016/j.ccr.2007.08.024.
132. Ovcharenko, V.I.; Vostrikova, K.E.; Romanenko, G. V; Ikorski, V.N.; Podberezskaya, N. V; Larionov, S. V Synthesis, Crystal Structure and Magnetic Properties of Di(Methanol) and Di(Ethanol)-Bis 2,2,5,5-Tetramethyl-1-Oxyl-3-Imidazoline-4-(3′,3′,3′-Trifluoromethyl-1-Propenyl-2′-Oxyato Nickel(II) - a New Type of Low Temperature Ferromagnetics. *Dokl. Akad. Nauk SSSR* **1989**, *306*, 115–118, doi:WOS:A1989U689100027.
133. Meng, X.; Shi, W.; Cheng, P. Magnetism in One-Dimensional Metal–Nitronyl Nitroxide Radical System. *Coord. Chem. Rev.* **2019**, *378*, 134–150, doi:10.1016/j.ccr.2018.02.002.
134. Fegy, K.; Vostrikova, K.E.; Luneau, D.; Rey, P. New Nitroxide Based Molecular Magnetic Materials. *Mol. Cryst. Liq. Cryst. Sci. Technol. Sect. A. Mol. Cryst. Liq. Cryst.* **1997**, *305*, 69–80, doi:10.1080/10587259708045047.
135. Ovcharenko, V.I.; Vostrikova, K.E.; Ikorskii, V.N.; Larionov, S. V; Sagdeev, R.Z. The Low Temperature Ferromagnet Dimethanol-Bis-[2,2,5,5-Tetramethyl-1-Oxyl-3-Imidazoline-4-(3′,3′,3′-Tri Fluoromethyl-1′-Propenyl-2′-Oxyato)] Cobalt(II), CoL2(CH3OH)2. *Dokl. Akad. Nauk SSSR* **1989**, *306*, 660–662, doi:WOS:A1989AC74400036.
136. Hintermaier, F.; Volodarsky, L.B.; Polborn, K.; Beck, W. New 2,5-Dihydroimidazole-1-Oxyls with Functional Side Groups (N, O, S Donors). *Liebigs Ann.* **1995**, *1995*, 2189–2194, doi: 10.1002/jlac.1995199512304.
137. Hintermaier, F.; Sünkel, K.; Volodarsky, L.B.; Beck, W. Synthesis, Structure, and Magnetic Properties of Transition Metal Complexes of the Nitroxide 2,5-Dihydro-4,5,5-Trimethyl-2,2-Bis(2-Pyridyl)Imidazole-1-Oxyl. *Inorg. Chem.* **1996**, *35*, 5500–5503, doi:10.1021/ic951345z.
138. Perfetti, M.; Caneschi, A.; Sukhikh, T.S.; Vostrikova, K.E. Lanthanide Complexes with a Tripodal Nitroxyl Radical Showing Strong Magnetic Coupling. *Inorg. Chem.* **2020**, *59*, 16591–16598, doi:10.1021/acs.inorgchem.0c02477.
139. Rey, P.; Smolentsev, A.I.; Vostrikova, K.E. Oxazolidine Nitroxide Transformation in a Coordination Sphere of the Ln3+ Ions. *Molecules* **2022**, *27*, 1626, doi:10.3390/molecules27051626.
140. Rey, P.; Caneschi, A.; Sukhikh, T.S.; Vostrikova, K.E. Tripodal Oxazolidine-N-Oxyl Diradical Complexes of Dy3+ and Eu3+. *Inorganics* **2021**, *9*, 91, doi:10.3390/inorganics9120091.
141. Köhn, R.D.; Pan, Z.; Kociok-Köhn, G.; Mahon, M.F. New Sandwich Complexes of Praseodymium(Iii) Containing Triazacyclohexane Ligands. *J. Chem. Soc. Dalt. Trans.* **2002**, 2344–2347, doi:10.1039/B110784B.
142. Wedal, J.C.; Ziller, J.W.; Evans, W.J. Trimethyltriazacyclohexane Coordination Chemistry of Simple Rare-Earth Metal Salts. *Dalt. Trans.* **2023**, *52*, 4787–4795, doi:10.1039/D3DT00242J.
143. Hazama, R.; Umakoshi, K.; Kabuto, C.; Kabuto, K.; Sasaki, Y. A Europium(III)-N,N,N′,N′-Tetrakis(2-Pyridylmethyl)-(R)-Propylenediamine Complex as a New Chiral Lanthanide NMR Shift Reagent for Aqueous Neutral Solution. *Chem. Commun.* **1996**, 15–16, doi:10.1039/CC9960000015.
144. Kira E. Vostrikova, Denis G. Samsonenko, CCDC 2268033: Experimental Crystal Structure Determination, DOI: 10.5517/ccdc.csd.cc2g42c2

145. Ishida, T.; Murakami, R.; Kanetomo, T.; Nojiri, H. Magnetic Study on Radical-Gadolinium(III) Complexes. Relationship between the Exchange Coupling and Coordination Structure. *Polyhedron* **2013**, *66*, 183–187, doi:10.1016/j.poly.2013.04.004.
146. Kanetomo, T.; Ishida, T. Strongest Exchange Coupling in Gadolinium(III) and Nitroxide Coordination Compounds. *Inorg. Chem.* **2014**, *53*, 10794–10796, doi:10.1021/ic501496a.
147. Kanetomo, T.; Yoshitake, T.; Ishida, T. Strongest Ferromagnetic Coupling in Designed Gadolinium(III)–Nitroxide Coordination Compounds. *Inorg. Chem.* **2016**, *55*, 8140–8146, doi:10.1021/acs.inorgchem.6b01072.
148. Hu, P.; Zhu, M.; Mei, X.; Tian, H.; Ma, Y.; Li, L.; Liao, D. Single-Molecule Magnets Based on Rare Earth Complexes with Chelating Benzimidazole-Substituted Nitronyl Nitroxide Radicals. *Dalt. Trans.* **2012**, *41*, 14651, doi:10.1039/c2dt31806g.
149. Wang, X.; Zhu, M.; Wang, J.; Li, L. Unusual Gd–Nitronyl Nitroxide Antiferromagnetic Coupling and Slow Magnetic Relaxation in the Corresponding Tb Analogue. *Dalt. Trans.* **2015**, *44*, 13890–13896, doi:10.1039/C5DT01487E.
150. Wang, J.; Miao, H.; Xiao, Z.-X.; Zhou, Y.; Deng, L.-D.; Zhang, Y.-Q.; Wang, X.-Y. Syntheses, Structures and Magnetic Properties of the Lanthanide Complexes of the Pyrimidyl-Substituted Nitronyl Nitroxide Radical. *Dalt. Trans.* **2017**, *46*, 10452–10461, doi:10.1039/C7DT01037K.
151. Benelli, C.; Caneschi, A.; Gatteschi, D.; Pardi, L. Gadolinium(III) Complexes with Pyridine-Substituted Nitronyl Nitroxide Radicals. *Inorg. Chem.* **1992**, *31*, 741–746, doi:10.1021/ic00031a010.
152. Hu, P.; Sun, Z.; Wang, X.; Li, L.; Liao, D.; Luneau, D. Magnetic Relaxation in Mononuclear Tb Complex Involving a Nitronyl Nitroxide Ligand. *New J. Chem.* **2014**, *38*, 4716–4721, doi:10.1039/C4NJ00627E.
153. Chen, P.Y.; Wu, M.Z.; Shi, X.J.; Tian, L. A Family of Multi-Spin Rare-Earth Complexes Based on a Triazole Nitronyl Nitroxide Radical: Synthesis, Structure and Magnetic Properties. *RSC Adv.* **2018**, *8*, 15480–15486, doi:10.1039/C8RA02546K.
154. Nakamura, T.; Ishida, T. Magnetic Exchange Interaction in Gadolinium(III) Complex Having Aliphatic Nitroxide Radical TEMPO.; 2016; p. 020016.
155. Caneschi, A.; Dei, A.; Gatteschi, D.; Sorace, L.; Vostrikova, K. Antiferromagnetic Coupling in a Gadolinium(III) Semiquinonato Complex. *Angew. Chemie - Int. Ed.* **2000**, *39*, doi:10.1002/(SICI)1521-3773(20000103)39:1<246::AID-ANIE246>3.0.CO;2-B.
156. Zheludev, A.; Barone, V.; Bonnet, M.; Delley, B.; Grand, A.; Ressouche, E.; Rey, P.; Subra, R.; Schweizer, J. Spin Density in a Nitronyl Nitroxide Free Radical. Polarized Neutron Diffraction Investigation and Ab Initio Calculations. *J. Am. Chem. Soc.* **1994**, *116*, 2019–2027, doi:10.1021/ja00084a048.
157. Hamada, D.; Fujinami, T.; Yamauchi, S.; Matsumoto, N.; Mochida, N.; Ishida, T.; Sunatsuki, Y.; Tsuchimoto, M.; Coletti, C.; Re, N. Luminescent DyIII Single Ion Magnets with Same N6O3 Donor Atoms but Different Donor Atom Arrangements, 'Fac'-[Dy^{III}(HLDL-Ala)$_3$]·8H_2O and 'Mer'-[Dy^{III}(HLDL-Phe)$_3$]·7H_2O. *Polyhedron* **2016**, *109*, 120–128, doi:10.1016/j.poly.2016.01.048.
158. Murakami, R.; Nakamura, T.; Ishida, T. Doubly TEMPO-Coordinated Gadolinium(III), Lanthanum(III), and Yttrium(III) Complexes. Strong Superexchange Coupling across Rare Earth Ions. *Dalt. Trans.* **2014**, *43*, 5893–5898, doi:10.1039/C3DT53586J.
159. Tkachenko, I.A.; Petrochenkova, N. V.; Mirochnik, A.G.; Karasev, V.E.; Kavun, V.Y. Carboxylato-Bis-Dibenzoylmethanates of Europium(III): Luminescence and Magnetic Properties. *Russ. J. Phys. Chem. A* **2012**, *86*, 681–684, doi: 10.1134/S0036024412040255.
160. Kahn, M.L.; Sutter, J.-P.; Golhen, S.; Guionneau, P.; Ouahab, L.; Kahn, O.; Chasseau, D. Systematic Investigation of the Nature of the Coupling between a Ln(III) Ion (Ln = Ce(III) to Dy(III)) and Its Aminoxyl Radical Ligands. Structural and Magnetic Characteristics of a Series of {Ln(Radical)$_2$} Compounds and the Related {Ln(Nitrone)$_2$} Derivat. *J. Am. Chem. Soc.* **2000**, *122*, 3413–3421, doi:10.1021/ja994175o.